STUDIES TOWARDS BIOCHEMICAL CHARACTERIZATION OF A NOVEL ACTIVITY FOR SIRTUIN 6

A Dissertation

Presented to the Faculty of the Graduate School

of Cornell University

In Partial Fulfillment of the Requirements for the Degree of

Doctor of Philosophy

by

Saba Khan

January 2014

© 2014 SABA KHAN

All rights reserved

STUDIES TOWARDS BIOCHEMICAL CHARACTERIZATION OF A NOVEL ACTIVITY FOR SIRTUIN 6

Saba Khan, Ph. D.

Cornell University 2014

One of the important posttranslational protein modifications is histone acetylation or deacetylation. Acetylation is catalyzed by the dedicated histone acetyltransferases and has been generally considered to be associated with transcription activation, while deacetylation is catalyzed by histone deacetylases (HDACs). One of the classes of HDACs called sirtuins are NAD^+-dependent deacetylases. There are seven sirtuins in mammals from Sirt1 – Sirt7. In this work, we study Sirt6, one of the sirtuins reported to have a weak deacetylase activity *in vitro*. However, Sirt6 has been involved in various important biological functions like life span expansion, genomic stability, transcriptional regulation, and metabolism. At the biochemical level, Sirt6 deacetylation has been attributed to most of these biological functions.

We found that human sirtuin Sirt6 can remove longer chain fattyacyl groups, such as myristoyl group, on the lysine residue much more efficiently than acetyl group. It is shown that this novel activity of Sirt6 allows it to accommodate more substrates other than H3K9. The catalytic efficiency for this new defattyacylase activity was found to be comparable to sirtuins with robust deacetylase activity. Further, the physiological relevance of this activity shows that Sirt6 promotes the secretion of TNFα by defattyacylating it at K19/K20 lysine residue.

BIOGRAPHICAL SKETCH

Saba Khan was born in Raipur and was brought up in Bilaspur, cities in the central part of India. She received her Master of Science degree in Chemistry and Chemical Biology from Cornell University in 2011 and her Integrated Master of Science in Chemistry from Indian Institute of Technology (IIT), Kharagpur in 2008. After her junior year at IIT, she spent the summer of 2006 at Dr. Reddy's Laboratory where she worked on the synthesis of oxozolidinones. She joined the Department of Chemistry and Chemical Biology at Cornell University in the fall of 2008 as a graduate student. At Cornell, she has been undergoing her doctoral research under the supervision of Professor Hening Lin. Her main research interests include chemical biology and biochemistry.

This document is dedicated to my family.

ACKNOWLEDGMENTS

My special thanks go to my thesis advisor Hening Lin. I have been privileged to pursue research under him, work with him as a teaching assistant, and learn the Advanced Chemical Biology in the class he taught. I am indebted to him for being such an inspiration and for guiding me all the way in my research.

I would also like to extend my thanks to the other committee members, Richard Cerione and Steven Ealick for their valuable suggestions and feedbacks which have helped me conduct this work. I would like to acknowledge other professors at Cornell whose classes have benefitted me: Tagdh Begley, Linda Nicholson, and Volker Vogt. I am also thankful to Patricia Hine for helping me out at various points during this works both academically and non-academically. My thanks also extend to the members of my lab: Xiaoyang Su, Anita Zhu, Hong Jiang, Jintang Du, Xuling Zhu, Bin He, Zhen Tong, Polly Aramsangtienchai, Jonathan Shrimp, Colleen Kuemmel, Ming Dong, and Huijing Hu. I am particularly thankful to Xiaoyang Su and Anita Zhu for being helpful in carrying out my research.

I would also like to thank other friends from Cornell: Nilanjan Bose, Ria Sircar, Parag Mahanti, Jimmy John, Swanpna Lekkala, Rachna Khurana, Amrita Harza, Asha Sharma, Swarnavo Sarkar, and Md. Saifur Rahman.

I would also like to thank Sujit Roy, my thesis advisor at IIT Kharagpur, for always encouraging me to do research.

Finally, I am extremely thankful to all my family members for being with me always.

TABLE OF CONTENTS

LIST OF FIGURES

LIST OF TABLES

CHAPTER 1

INTRODUCTION

1.1 Posttranslational Modification and its Immediate Biological Implications

The global set of proteins produced by an organism is called the *proteome.* It results firstly from the direct translation of the genome, secondly from the diversification at the mRNA level (either through alternative splicing at the mRNA level or by using alternative promoter sequence), and thirdly by the diversification of the translated protein through covalent modifications. The chemical modification of the protein either by the covalent addition of small molecules to the amino acid side chain or the hydrolytic cleavage of peptide bond(s) of the protein is broadly termed as *posttranslational modification* (PTM). Some of the direct consequences of PTMs result in the following functional changes in proteins (1):

1) activation/deactivation of the protein catalytic activity,
2) change in the localization of proteins, and
3) change in protein-protein interactions.

The examples of PTMs and their biological implications are numerous. Ser/Thr/Tyr phosphorylation is known to be involved in inducing the signal transduction pathways either by switching its catalytic activity or by producing binding sites for the partners (2). Lysine methylation and acetylation on histones regulate gene transcription (3). The fattyacylation of proteins, namely N-myristoylation and S-palmitoylation, are responsible for membrane targeting of proteins (4). Protein polyubiquitylation helps in

protein degradation, endocytosis, and cell signaling (5, 6). These are just a few examples that show that PTMs are involved in many important biological processes.

1.2 Lysine Acetylation – Histone Acetyltransferases (HATs)

Lysine acetylation is an important PTM that is involved in regulating the transcription of genes associated with histones. The acetylation of histones is catalyzed by a family of proteins called *histone acetyltransferases* (HATs) and is considered to be associated with transcriptional activation. In addition to histones, lysine acetylation has been reported to occur in several other proteins (7-10). Recently, several novel acyl lysine modifications have been discovered. A few examples of such modifications include propionylation, butyrylation, crotonoylation, succinylation, malonylation, and myristoylation (11).

1.3 Lysine Deacetylation – Histone Deacetylases (HDACs)

The deacetylation of histones is catalyzed by another family of proteins called *histone deacetylases* (HDACs) and is associated with transcriptional silencing (12). HDACs keep these lysine side chains hypoacetylated, thereby condensing the chromosomes and keeping the transcriptional machinery shut down (1, 13).

There are eighteen HDACs in mammals which are divided into four classes, namely class I-IV, based on their sequence homology to yeast Sir2. Classes I, II, and IV are commonly known as *classical* HDACs and comprise eleven members. Class III HDACs are called "*sirtuins*" and there are seven sirtuins in mammals. Classical HDACs differ from sirtuins in their catalytic mechanism for the deacetylation of histones. The

HDACs make use of Zn^{+2} ion in the catalytic pocket and act as metal dependent amide-hydrolases, whereas sirtuins use nicotinamide adenine dinucleotide (NAD^{+}) cofactor as a co-substrate to hydrolyze the acetyl group from the side chain lysine of histones – the detailed mechanism of the same is discussed in the next section.

1.3.1 Sirtuins

The founding member of the sirtuin family is the yeast Sir2 (Silent Mating Type Information Regulator), which has been known to be a silencing factor. The histone deacetylase activity of the yeast Sir2 has been attributed to gene silencing. Also, it has been shown to be responsible for the life span expansion of yeast during the caloric restriction (14-16). The simple phylogenetic classification (17) of sirtuins in different species is shown in Fig. 1.1.

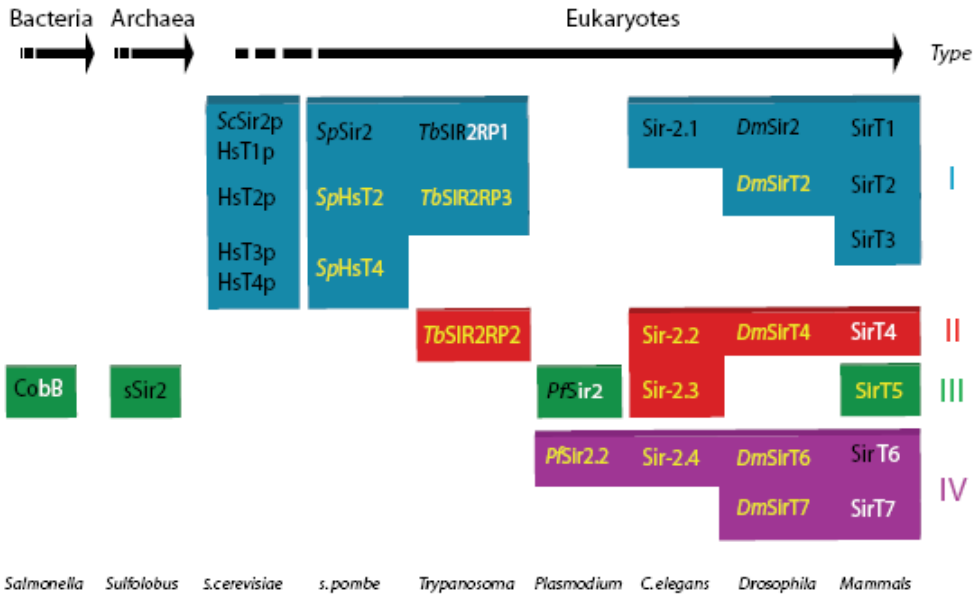

Fig. 1.1 Phylogenetic classification of sirtuins in bacteria, archaea, and eukaryotes: the white and black letterings of figure signify the associated deacetylation and ADP-ribosyl transferase activity. (Figure taken from Int. J. Dev. Biol. 53, 303-322 (2009)).

The functions of sirtuins are conserved from archaea to eukaryotes, so these phylogenetic trees are helpful in inferring a new activity for sirtuins from one species to a different species.

Mammalian sirtuins, Sirt1-7, based on their sequence similarity have been grouped roughly in four classes: Sirt1, Sirt2, and Sirt3 form class I, Sirt4 is class II, Sirt5 is class III, and Sirt6 and Sirt7 are class IV sirtuins. Sirtuins have been reported earlier to be found in different sub-cellular localizations. Sirt1, Sirt6, and Sirt7 are found in the nucleus, Sirt2 is found in the cytosol, and Sirt3, Sirt4, and Sirt5 are found in the mitochondria. However, there are reports including some work from our research group indicating that localizations might be different from that stated above (18). All mammalian sirtuins have been thought to be NAD^+-dependent histone deacetylases. The most accepted mechanism of deacetylation is shown in Fig. 1.2. The mechanism has been extensively studied (19-26). It can be described as a two step process, which proceeds firstly with the acetyl oxygen attacking the anomeric carbon of the sugar back bone, releasing nicotinamide as a by-product and forming an α-1´-O-alkylimidate intermediate. The 2´-OH then attacks the intermediate, followed by hydrolysis to give the 2´-O-acetyl-ADP-ribose (O-Ac-ADPR), which can isomerize to form 3´-O-Ac-ADPR non-enzymatically. A conserved histidine residue has been shown to be involved in the catalysis.

Sirtuins have been reported to be involved in a number of biological functions. These functions include the regulation of life span, transcription, apoptosis, genome stability, and metabolism (27-29).

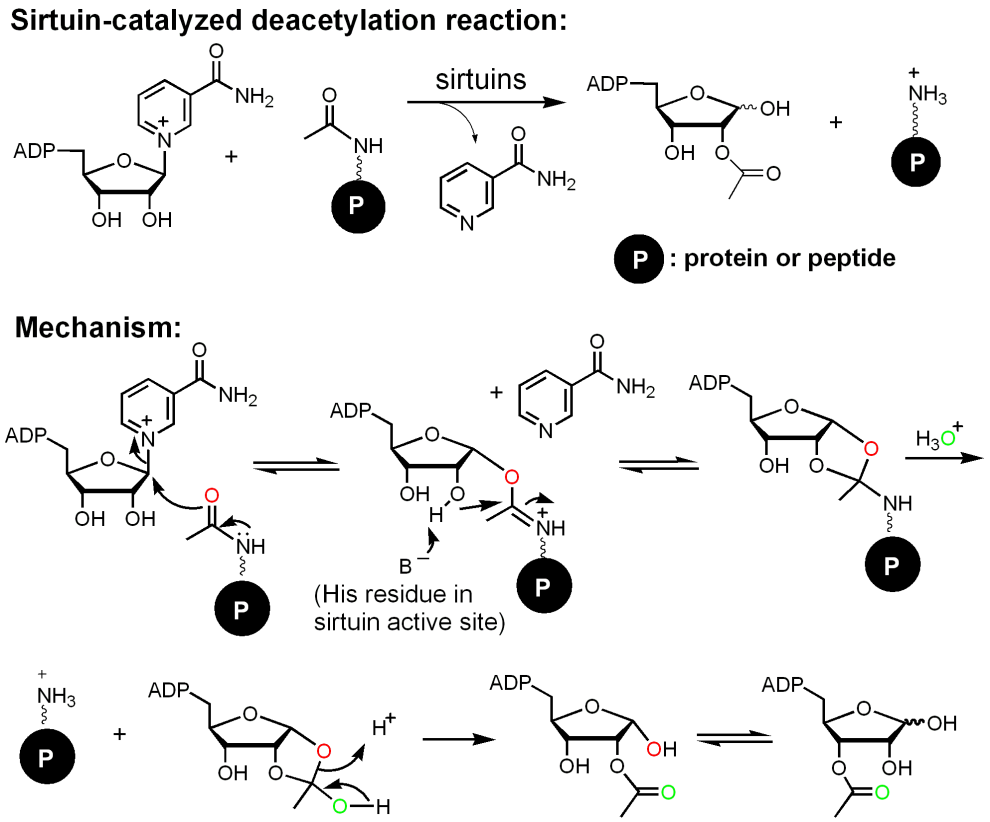

Fig. 1.2 Sirtuin catalyzed NAD-dependent deacetylation reaction and the most accepted mechanism.

1.3.2 Crystal Structure of Sirtuins

The crystal structure of different sirtuins with various ligands has been reported (30). Sirtuins typically contain Zn^{+2} coordinated by four conserved cysteine residues. The Zn^{+2} ion is necessary for keeping the structure intact. There are two domains in the crystal structure: a smaller Zn^{+2} binding domain and the larger domain containing a Rossmann fold for binding NAD^{+} (Fig. 1.3). The N and C termini vary in the sequence whereas the core catalytic domain is more or less conserved in sirtuins. The large and the small domains are connected through loops in such a way that a cleft is formed, which is where the substrate and NAD^{+} bind the protein from the opposite directions.

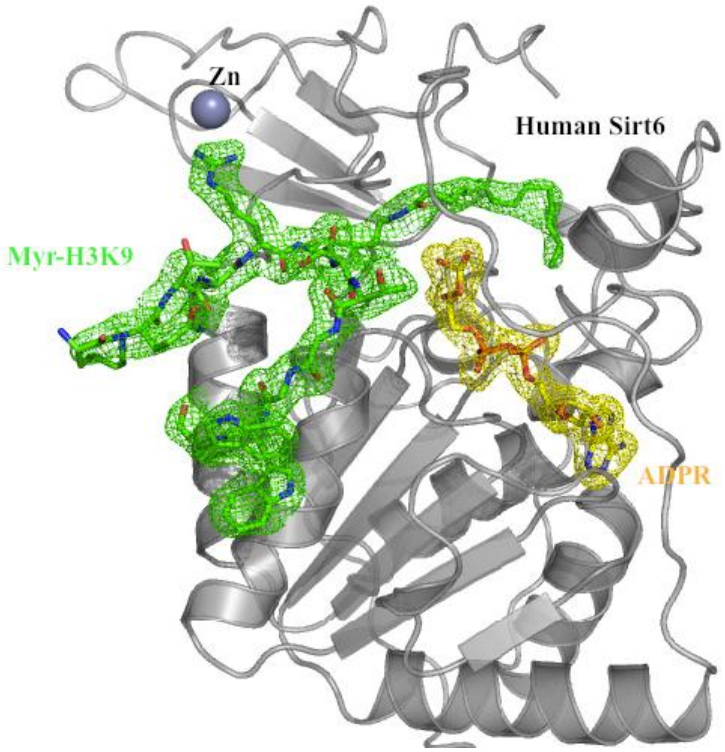

Fig. 1.3 Overall crystal structure of Sirt6 with Myr-H3K9 peptide (in green) and ADPR (in yellow) which binds at the same position as NAD^+.

1.4 Motivation and Prior Work on Sirtuin 6

At the biochemical level, only a few sirtuins have robust deacetylation activity. For instance, Sirt1, Sirt2, and Sirt3 have been reported to exhibit robust deacetylation activity. Sirt4 has no deacetylation activity (31, 32). On the other hand, Sirt5 (33, 34), Sirt6 (35), and Sirt7 (32) have been known to have very weak deacetylation activity. The gap between important biological activities and the lack of robust deacetylation activity prompted us to think that the sirtuins with the weak deacetylase activity might remove other physiologically relevant modification on the lysine residue.

Du *et al.* demonstrated that the above hypothesis is indeed true in human Sirt5 (36). They showed that Sirt5 removes the malonyl and succinyl modifications on lysine residues much more efficiently than the deacetylation activity and that protein succinylation and malonylation occur in cells. Based on the information from the crystal structure of Sirt5 with thioacetyl peptide, they predicted that if the acetyl group is replaced with an acyl group bearing a negatively charged carboxylate ion, the acyl peptide would bind Sirt5 better than the acetyl peptide. Therefore, such modifications might be better substrates for Sirt5. Du *et al.* further tested the malonyl and succinyl modifications on various peptides as the physiologically relevant substrates for Sirt5. This was the first evidence that a sirtuin could preferentially remove an acyl modification other than the known acetyl group more efficiently. This work made us think that Sirt6, which was reported to have a weak deacetylase activity, could also prefer to hydrolyze other acyl modifications. In this thesis, we have proved this hypothesis by showing that Sirt6 prefers to hydrolyze medium and long chain fattyacyl groups.

1.4.1 Sirt6 Prior Work

A brief mention of prior work on Sirt6 is important to establish the necessity for exploring the new activity of Sirt6, which has been reported to be a nuclear protein (32). Sirt6 is known to possess two weak biochemical activities namely ADP-ribosyltransferase activity and deacetylation activity. Although weak, both activities have important biological functions as described below.

Sirt6 has been reported to possess mono-ADP-ribosyltransferase activity. At the biochemical level, this happens when sirtuins transfer ADP-ribose moiety of NAD^+ to

other proteins. Earlier, Sirt6 was found to ADP-ribosylate itself. However this activity was thought to be weak. (37). Du *et al.* showed by using the NAD analogues that this activity might be too weak to be physiologically relevant (38). Recently, it has been demonstrated that during oxidative stress, Sirt6 ADP-ribosylates PARP-1 and promotes DNA repair (39). This activity has also been attributed to the role of Sirt6 in inducing massive apoptosis in the cancerous cells selectively (40).

Sirt6 has been reported to have sequence specific weak deacetylase activity on H3K9 and H3K56 histone substrates (35, 41, 42). Most of the biological functions of Sirt6 have been associated to this weak deacetylase activity. However, no measurement of its enzymatic efficiency (i.e. k_{cat}, K_m) has been reported so far. The various biological functions have been elaborated below in which deacetylation activity of Sirt6 has been thought to be involved.

Aging

It has been shown that Sirt6 over expression increases the life span of the male mice. Sirt6 knock out (KO) mice were reported to show the phenotype of aging (43). On cellular levels, studies have shown that Sirt6 knock down (KD) cells show increased genomic instability, susceptibility towards ionizing radiation, phenotype of defective base excision repair (BER), and DNA double-strand break (DSB) repair.

Metabolism

Recent work by Mostoslavasky *et al.* (44) demonstrated that Sirt6 is a corepressor of hypoxia-inducible factor 1-alpha **(**Hif1α) gene. The overexpression of Sirt6 was shown

to down regulate the various glycolytic genes. Sirt6 deficient mice were shown to suffer from acute hypoglycemia. All these results indicate that Sirt6 is an important player in glucose metabolism. In another finding, Sirt6 has also been shown to promote fat utilization by fatty acid oxidation in wildtype mice. It has been shown that Sirt1, FOXO3a, and NRF1 form a complex and positively regulate Sirt6 gene expression, which in turn negatively regulates glycolysis, triglyceride synthesis, and fat metabolism. Sirt6 has been shown to deacetylate H3K9 in the promoter region of the genes involved in glycolysis, triglyceride synthesis and fat metabolism (45).

Genome Stability and Sirtuins

Sirt6 has been reported to be important in maintaining telomere integrity by deacet lating H3K9 and H3K56 histone sequences (35). Telomeres are sequences at the end of chromosomes and provide protection from aberrant DNA repair, fusion, and degradation of the chromosome ends. Sirt6 depletion leads to abnormal telomere metabolism. Genomic stability is also maintained by Sirt6 mediated DNA repair. It is important at the DNA DSB repair sites because it induces structural changes in chromatin at these DSB sites, which is essential for the efficient association of DSB repair proteins (46). DNA dependent protein kinase or DNA-PK is one such example of DSB repair protein. DNA-PK is a non-homologous end joining (NHEJ) holoenzyme, which in turn repairs DSBs using an NHEJ mechanism. Sirt6 has also been reported to promote DSB repair through homologous recombination which happens in two steps firstly by activating PARP-1, and secondly by deacetylating and thereby activating the end resection protein called CtIP.

Inflammation Response

NF-κB has been known to be a key transcription factor in aging, proliferation, and for the control of inflammation response genes (47). It was recently reported that Sirt6 interacts with NF-κB physically and is recruited to the promoters of several NF-κB target genes by deacetylating these promoters at the H3K9 position, and thereby decreasing the NF-κB signaling (48).

1.5 Connection between TNFα and Sirt6

The involvement of Sirt6 in regulating the synthesis of the tumor necrosis factor α (TNFα) in a NAD^+ dependent manner has been demonstrated by two research groups (49, 50). TNFα is a type II membrane protein that is known to be involved in systemic inflammation. It is central to many signaling pathways like NF-κB and mitogen-activated protein kinase **(**MAPK) pathway. TNFα has been shown to be myristoylated at K19 and K20 residues (51, 52). While exploring the new enzymatic activity for Sirt6 (as described in Section 1.4), we discovered that Sirt6 possesses a novel defattyacylase activity. That is, it prefers to remove longer chain fattyacyl group modification on histone peptides. We made use of the above information and demonstrated that Sirt6 might affect the TNFα secretion by defattyacylating it. The details of our approach are described in the next section.

1.6 My Dissertation Statement

My dissertation work investigates the class IV sirtuin, Sirt6, which has been reported to be important for DNA repair, transcriptional regulation of genes involved in

metabolism and inflammation, genome stability, and for life span expansion. Almost all the biological functions of Sirt6 have been attributed to its weak and site specific histone deacetylase activity. My goal was to look for alternate acyl lysine modifications which might be removed by Sirt6. I showed that Sirt6 hydrolyzes longer chain acyl modifications much more efficiently than the short acetyl modification on lysine residues of the histone peptide. Therefore, defattyacylation is a novel Sirt6 activity.

In Chapter 2, I present biochemical and enzymology data establishing a novel activity for Sirt6 which is much more efficient than the previously reported weak deacetylase activity, which was thought to be responsible for its myriad biological functions. Using various biochemical techniques such as HPLC coupled with mass spectroscopy, I demonstrated that Sirt6 shows preference for removing longer chain acyl modifications in comparison to other physiologically relevant modifications such as biotin, hydroxyl methyl glutaryl (HMG) succinyl, lipoyl, acetyl, ubiquitinyl, and SUMOyl (small peptide sequences from ubiquitin and SUMO peptide) on Lys9 of the H3K9 peptide. I further determined that Sirt6 removes myristoyl group from the H3K9 peptide approximately 300 fold better than its acetyl counterpart.

Also, I used HPLC based techniques to show that this more efficient activity also allows Sirt6 to utilize substrates other than H3K9acetyl peptide. Using autoradiography, HPLC, and MALDI-TOF mass spectroscopy, I showed that the reaction mechanism for this novel Sirt6 "*demyristoylase*" activity is the same as that which has been established for deacetylase activity. The preference for longer chain fattyacyl group has been demonstrated using the crystal structure of Sirt6 with H3K9myr peptide and ADP-ribose. This chapter also includes some of my efforts towards determining whether or not

histones have these long chain fattyacyl modifications. It also includes a brief acknowledgement to the work of my colleague Hong Jiang in establishing the physiological relevance for demyristoylase activity of Sirt6. In summary, he showed that Sirt6 promotes the secretion of TNFα by removing the fattyacyl modification on Lys19/20 of TNFα. To corroborate this at the biochemical level, using HPLC based *in vitro* activity assay, I showed that Sirt6 could indeed remove myristoyl groups from Lys19 and Lys20 of a synthetic TNFα peptide. Also, I obtained kinetic data using HPLC based assays to show that the demyristoylation of TNFα K19myr and TNFα K20myr peptides was as efficient as deacetylase activity of sirtuins Sirt1-3, which exhibit robust deacetylation activity. Some of these results are also available in reference (53).

In Chapter 3, I present possible extensions and some of the incomplete work on Sirt6. Firstly, my goal was to clone and express the Sirt6 mutant that would abrogate the defattyacylation activity. We made use of the crystal structure to identify four such residues, Leu9, Val115, Phe82, and Phe86 that were in close interaction with the hydrophobic myristoyl chain. I was able to mutate and express three of them, Leu9, Val115, and Phe82, to more hydrophilic arginine residue. Further studies need to be done for the activity of these mutated proteins with TNFα myristoyl peptides and H3K9 myristoyl peptides to confirm which one abrogates the defattyacylation activity. The chapter also includes some proposed experiments to explore how the recently reported ADP-ribosyl transferase activity of Sirt6 might affect our defattyacylase activity.

Chapter 4 provides important concluding remarks, briefs about the significance of this work, and presents a few future directions that we can pursue based on this work.

REFERENCES

1. Walsh, C. T., Posttranslational Modification of Proteins: Expanding Nature's Inventory. Roberts and Company Publishers, Englewood, Colorado (2005).
2. Johnson, L. N. and Lewis, R. J., Structural Basis for Control by Phosphorylation. *Chem. Rev.* 101, 2209-2242 (2001).
3. Jenuwein, T. and Allis, C. D., Translating the Histone Code. *Science* 293, 1074-1080 (2001).
4. Resh M. D., Fattyacylation of Protein: New Insights into Membrane Targeting of Myristoylated and Palmitoylated Proteins. *Biochem. Biophys. Acta* 1451, 1-16 (1999).
5. Kerscher, O., Felberbaum, R. and Hochstrasser, M., Modification of Proteins by Ubiquitin and Ubiquitin-Like Proteins. *Annu. Rev. Cell Dev. Biol.* 22, 159-180 (2006).
6. Mukhopadhyay, D. and Riezman, H., Proteasome-Independent Functions of Ubiquitin in Endocytosis and Signaling. *Science* 315, 201-205 (2007).
7. Zhao, S., Xu, W., Jiang, W., Yu, W., Lin, Y., Zhang, T. *et al*., Regulation of Cellular Metabolism by Protein Lysine Acetylation. *Science* 327, 1000-1004 (2010).
8. Wang, Q., Zhang, Y., Yang, C., Xiong, H., Lin, Y., Yao, J. *et al*., Acetylation of Metabolic Enzymes Coordinates Carbon Source Utilization and Metabolic Flux. *Science* 327, 1004-1007 (2010).

9. Schwer, B., Bunkenborg, J., Verdin, R. O., Andersen, J. S. and Verdin, E., Reversible Lysine Acetylation Controls the Activity of the Mitochondrial Enzyme Acetyl-CoA Synthetase 2. *Proc. Natl. Acad. Sci. U. S. A.* 103, 10224-10229 (2006).
10. Starai, V. J., Celic, I., Cole, R. N., Boeke, J. D. and Escalante-Semerena, J. C., Sir2-Dependent Activation of Acetyl-CoA Synthetase by Deacetylation of Active Lysine. *Science* 298, 2390-2392 (2002).
11. Su, X., He B., and Lin, H., Protein Lysine Acylation and Cysteine Succination by Intermediates of Energy Metabolism. *ACS Chem. Bio.* 7(6), 947-60, June 15 (2012).
12. Shahbazian, M. D. and Grunstein, M., Functions of Site-Specific Histone Acetylation and Deacetylation. *Annu. Rev. Biochem.* 76, 75-100 (2007).
13. Verdin, E., Dequiedt, F., and Kasler, H. G., Class II Histones Deacetylases: Versatile Regulators. *Trends Genet.* 19, 286-294 (2003).
14. Kaeberlein, M., McVey, M., and Guarente, L., The SIR2/3/4 Complex and SIR2 Alone Promote Longevity in Saccharomyces Cerevisiae by Two Different Mechanisms. *Genes Dev.* 13, 2570-2580 (1999).
15. Lin, S. J., Defossez, P. A., and Guarente, L., Requirement of NAD and SIR2 for Life-Span Extension by Calorie Restriction in Saccharomyces Cerevisiae. *Science* 289, 2126-2128 (2000).
16. Imai, S.-I., Armstrong, C. M., Kaeberlein, M. and Guarente, L., Transcriptional Silencing and Longevity Protein Sir2 is an NAD-Dependent Histone Deacetylase. *Nature* 403, 795-800 (2000).

17. Vaquero, A., The Conserved Role of Sirtuins in Chromatin Regulation. *Int. J. Dev. Biol.* 53, 303-322 (2009).

18. Schber, M. B., Vaquero, A., and Reinberg, D., SirT3 is a Nuclear NAD-Dependent Histone Deacetylase that Translocates to the Mitochondria upon Cellular Stress. *Genes Dev.* 21, 920-928 (2007).

19. Tanner, K. G., Landry, J., Sternglanz, R. and Denu, J. M., Silent Information Regulator 2 Family of NAD-Dependent Histone/Protein Deacetylases Generates a Unique Product, 1-O-Acetyl-ADP-Ribose. *Proc. Natl. Acad. Sci. U. S. A.* 97, 14178-14182 (2000).

20. Tanny, J. C. and Moazed, D., Coupling of Histone Deacetylation to NAD Breakdown by the Yeast Silencing Protein Sir2: Evidence for Acetyl Transfer from Substrate to an NAD Breakdown Product. *Proc. Natl. Acad. Sci. U. S. A.* 98, 415-420 (2001).

21. Sauve, A. A., Celic, I., Avalos, J., Deng, H., Boeke, J. D., and Schramm, V. L., Chemistry of Gene Silencing: The Mechanism of NAD^+-Dependent Deacetylation Reactions. *Biochemistry* 40, 15456-15463 (2001).

22. Jackson, M. D. and Denu, J. M., Structural Identification of 2´- and 3´-O-Acetyl-ADP-Ribose as Novel Metabolites Derived from the Sir2 Family of Beta-NAD^+-Dependent Histone/Protein Deacetylases. *J. Biol. Chem.* 277, 18535-18544 (2002).

23. Jackson, M. D., Schmidt, M. T., Oppenheimer, N. J., and Denu, J. M., Mechanism of Nicotinamide Inhibition and Transglycosidation by Sir2 Histone/Protein Deacetylases. *J. Biol. Chem.* 278, 50985-50998 (2003).

24. Smith, B. C. and Denu, J. M., Sir2 Protein Deacetylases: Evidence for Chemical Intermediates and Functions of a Conserved Histidine. *Biochemistry* 45, 272-282 (2006).

25. Smith, B. C. and Denu, J. M., Sir2 Deacetylases Exhibit Nucleophilic Participation of Acetyl-lysine in NAD^+ Cleavage. *J. Am. Chem. Soc.* 129, 5802-5803 (2007).

26. Sauve, A. A. and Schramm, V. L., Sir2 Regulation by Nicotinamide Results from Switching between Base-Exchange and Deacetylation Chemistry. *Biochemistry* 42, 9249-9256 (2003).

27. Carlos, S., Satterstrom, F. K., Haigas, M., and Mostoslavasky, R., From Sirtuin Biology to Human Diseases: An Update. *J. Bio. Chem.* vol. 287, no. 51, 42444-42452 (2012).

28. Michan, S. and Sinclair, D., Sirtuins in Mammals: Insights into Their Biological Function. *Biochem. J.* 404, 1-13 (2007).

29. Houtkooper, R. H., Pirinen, E., and Auwerx, J., Sirtuins as Regulators of Metabolism and Health Span., *Nat. Rev. Mol. Cell Biol.* 13, 225-238 (2012).

30. Yuan, H. and Marmorstein, R., Structural Basis for Sirtuin Activity and Inhibition. *J. Bio. Chem.* 287, 42428-42435 (2012).

31. Haigis, M. C., Mostoslavsky, R., Haigis, K. M., Fahie, K., Christodoulou, D. C., Murphy, A. J. *et al*., SIRT4 Inhibits Glutamate Dehydrogenase and Opposes the Effects of Calorie Restriction in Pancreatic β Cells. *Cell* 126, 941-954 (2006).

32. Michishita, E., Park, J. Y., Burneskis, J. M., Barrett, J. C., and Horikawa, I., Evolutionarily Conserved and Non-Conserved Cellular Localizations and Functions of Human SIRT Proteins. *Mol. Biol. Cell* 16, 4623-4635 (2005).

33. Schuetz, A., Min, J., Antoshenko, T., Wang, C.-L., Allali-Hassani, A., Dong, A. *et al*., Structural Basis of Inhibition of the Human NAD^{+}-Dependent Deacetylase SIRT5 by Suramin. *Structure* 15, 377-389 (2007).

34. Schlicker, C., Gertz, M., Papatheodorou, P., Kachholz, B., Becker, C. F. W., and Steegborn, C., Substrates and Regulation Mechanisms for the Human Mitochondrial Sirtuins SirT3 and SirT5. *J. Mol. Biol.* 382, 790-801 (2008).

35. Michishita, E., McCord, R. A., Berber, E., Kioi, M., Padilla-Nash, H., Damian, M. *et al*., SIRT6 is a Histone H3 Lysine 9 Deacetylase that Modulates Telomeric Chromatin. *Nature* 452, 492-496 (2008).

36. Du, J., Zhou, Y., Su, X., Yu, J. J., Khan, S., Jiang, H., Kim, J., Woo, J., Kim, J. H., Choi, B. H., He, B., Chen, W., Zhang, S., Cerione, R. A., Auwerx, J., Hao, Q., and Lin, H., SirT5 is a NAD-Dependent Protein Lysine Demalonylase and Desuccinylase. *Science* 334, 806–809 (2011).

37. Liszt, G., Ford, E., Kurtev, M., and Guarente, L., Mouse Sir2 Homolog SIRT6 is a Nuclear ADP-Ribosyltransferase. *J. Biol. Chem.* 280, 21313-21320 (2005).

38. Du, J., Jiang, H., and Lin, H., Investigating the ADP-Ribosyltransferase Activity of Sirtuins with NAD Analogs and ^{32}P-NAD. *Biochemistry* 48, 2878-2890 (2009).

39. Mao Z, Hine C., Tian X., Van Meter M., Au M., Vaidya A., Seluanoy A., and Gorbunova V., SIRT6 Promotes DNA Repair under Stress by Activating PARP-1. *Science* 17, 332 (6036):1443-6, June (2011).

40. Van, M. M., Mao, Z., Gorbunova, V., and Seluanov, A., SIRT6 Overexpression Induces Massive Apoptosis in Cancer Cells But Not in Normal Cells. *Cell Cycle*, 10(18): 3153-8 (2011).

41. Yang, B., Zwaans, B. M. M., Eckersdorff, M., and Lombard, D. B., The Sirtuin SIRT6 Deacetylates H3 K56Ac in vivo to Promote Genomic Stability. *Cell Cycle* 8, 2662-2663 (2009).

42. Michishita, E., McCord, R. A., Boxer, L. D., Barber, M. F., Hong, T., Gozani, O. *et al.*, Cell Cycle-Dependent Deacetylation of Telomeric Histone H3 Lysine K56 by Human SIRT6. *Cell Cycle* 8, 2664-2666 (2009).

43. Kanfi, Y., Naiman, S., Amir, G., Peshti, V., Zinman, G., Nahum, L., Bar-Joseph, Z., and Cohen, H. Y., The Sirtuin SIRT6 Regulates Lifespan in Male Mice. *Nature* 483, 218-221 (2012)

44. Zhong, L., D'Urso, A., Toiber, D., Sebastian, C., Henry, R. E., Vadysirisack, D. D., Guimaraes, A., Marinelli, B., Wikstrom, J. D., Nir, T., Clish, C. B., Vaitheesvaran, B., Iliopoulos, O., Kurland, I., Dor, Y., Weissleder, R., Shirihai, O. S., Ellisen, L. W., Espinosa, J. M., and Mostoslavsky, R., The Histone Deacetylase Sirt6 Regulates Glucose Homeostasis via Hif1 α. *Cell* 140, 280-293 (2010).

45. Kim, H. S., Xiao, C., Wang, R. H., Lahusen, T., Xu, X., Vassilopoulos, A., Vazquez-Ortiz, G., Jeong, W. I., Park, O., Ki, S. H., Gao, B., and Deng, C. X., Hepatic-Specific Disruption of SIRT6 in Mice Results in Fatty Liver Formation due to Enhanced Glycolysis and Triglyceride Synthesis. *Cell Metab.* 12, 224-23 (2010).

46. McCord, R. A., *et al*., SIRT6 Stabilizes DNA-Dependent Protein Kinase at Chromatin for DNA Double-Strand Break Repair. *Aging.* 1, 109-121 (2009).

47. Hayden, M. S., and Ghosh, S., Shared Principles in NF-kappaB Signaling. *Cell* 132 (3), 344-62, Feb. 8 (2008).

48. Kawahara, T. L., *et al*., SIRT6 Links Histone H3 Lysine 9 Deacetylation to NF-kappaB-Dependent Gene Expression and Organismal Life Span. *Cell* 136, 62-74 (2009)

49. Bruzzone, S., Fruscione, F., Morando, S., Ferrando, T., Poggi, A., Garuti, A. *et al*., Catastrophic NAD Depletion in Activated T Lymphocytes through Nampt Inhibition Reduces Demyelination and Disability in EAE. *PLoS ONE* 4, e7897 (2009).

50. Van Gool, F., Galli, M., Gueydan, C., Kruys, V., Prevot, P.-P., Bedalov, A. *et al*., Intracellular NAD Levels Regulate Tumor Necrosis Factor Protein Synthesis in a Sirtuin-Dependent Manner. *Nat. Med.* 15, 206-210 (2009).

51. Stevenson, F. T., Bursten, S. L., Locksley, R. M., and Lovett, D. H., Myristyl Acylation of the Tumor Necrosis Factor Alpha Precursor on Specific Lysine Residues. *J. Exp. Med.* 176, 1053-1062, (1992).

52. Stevenson, F. T., Bursten, S. L., Fanton, C., Locksley, R. M., and Lovett, D. H., The 31-kDa Precursor of Interleukin 1 Alpha is Myristoylated on Specific Lysines within the 16-kDa N Terminal Propiece. *Proc. Natl. Acad. Sci. U. S. A.* 90, 7245-7249 (1993).

53. Jiang, H., Khan, S., Wang, Y., Charron, G., He, B., Sebastian, C., Du, J., Kim, R., Mostoslavasky, R., Hang, H. C., Hao, Q., and Lin, H., Sirt6 Regulates TNFα via

Hydrolysis of Long Chain Fatty Acyl Lysine. *Nature* 496, 110-113, April 4 (2013).

CHAPTER 2

Sirt6 Regulates TNF-Secretion via Hydrolysis of Long Chain Fattyacyl Lysine

2.1 Abstract

The Sir2 family of enzymes (sirtuins) is known as nicotinamide adenine dinucleotide (NAD)-dependent deacetylases. However, four of the seven mammalian sirtuins including Sirt5 and Sirt6 have very weak or no deacetylase activity *in vitro*. Recently, it has been shown that Sirt5 possesses robust lysine desuccinylase and demalonylase activities *in vitro*. In this work, I show that human Sirt6 can efficiently remove long chain fattyacyl groups such as myristoyl from lysine residues in histone peptides. This novel activity further supports the statement that sirtuins are "NAD-dependent deacylases" rather than commonly called NAD-dependent deacetylases. The crystal structure of Sirt6 discloses a large hydrophobic pocket that can accommodate long chain fattyacyl groups. Further, it has been demonstrated that Sirt6 could regulate TNFα secretion achieved by defattyacylating the previously reported K19/K20 myristoyl group on TNFα.

2.2 Introduction

Sirtuins are ancient family of proteins that are present in all life forms and exhibit a conserved structure and catalytic activity from bacteria to mammals. The first discovered member called as Sir2 (Silent mating type Information Regulator factor 2) in yeast, was identified as gene for silencing chromatin by working at the biochemical level as a histone deacetylase (1). The catalytic activity of the sirtuin family of proteins has

been attributed to their NAD^+ cofactor dependent histone deacetylase activities (2, 3). Seven sirtuins, namely Sirt1 to Sirt7, found in mammals have been shown to be involved in various biological functions such as regulation of life span (4-8), genome stability (9), transcription (10-13), and metabolism (14-18).

Four of the seven mammalian sirtuins including Sirt5 and Sirt6 have been reported to have very weak or no detectable deacetylase activity (19-22). Using the enzymology data and crystal structure, Du *et al.* recently showed that Sirt5 hydrolyzes malonyl and succinyl peptides much efficiently than the corresponding acetyl peptide on lysine residues (23). The Sirt5 catalyzed deacylation reaction and its mechanism are shown in Fig. 2.1. This finding was further corroborated by Zhang *et al.* who showed that many mammalian proteins are succinylated or malonylated (24). This new activity of Sirt5 led us to hypothesize that other sirtuins with weak deacetylase activity could also hydrolyze other acyllysine modifications.

In this work, I specifically studied Sirt6 to explore whether it has any new activity. The biological functions of Sirt6 have been well described in literature (25-30). In most cases, the biological functions have been linked to the sequence specific deacetylase activity of Sirt6 on histone H3K9 and H3K56 peptide sequences, but not on other histone sequences. In this work, I found a novel activity for Sirt6. In particular, using the enzymology data, I established that Sirt6 prefers to hydrolyze longer chain fattyacyl modifications better than the shorter acetyl modification on lysine residues. In terms of the catalytic efficiency (k_{cat}/K_m), this new activity is comparable to other sirtuins with robust deacetylation activity (for example Sirt1-3). The sequence specificity of Sirt6 is in

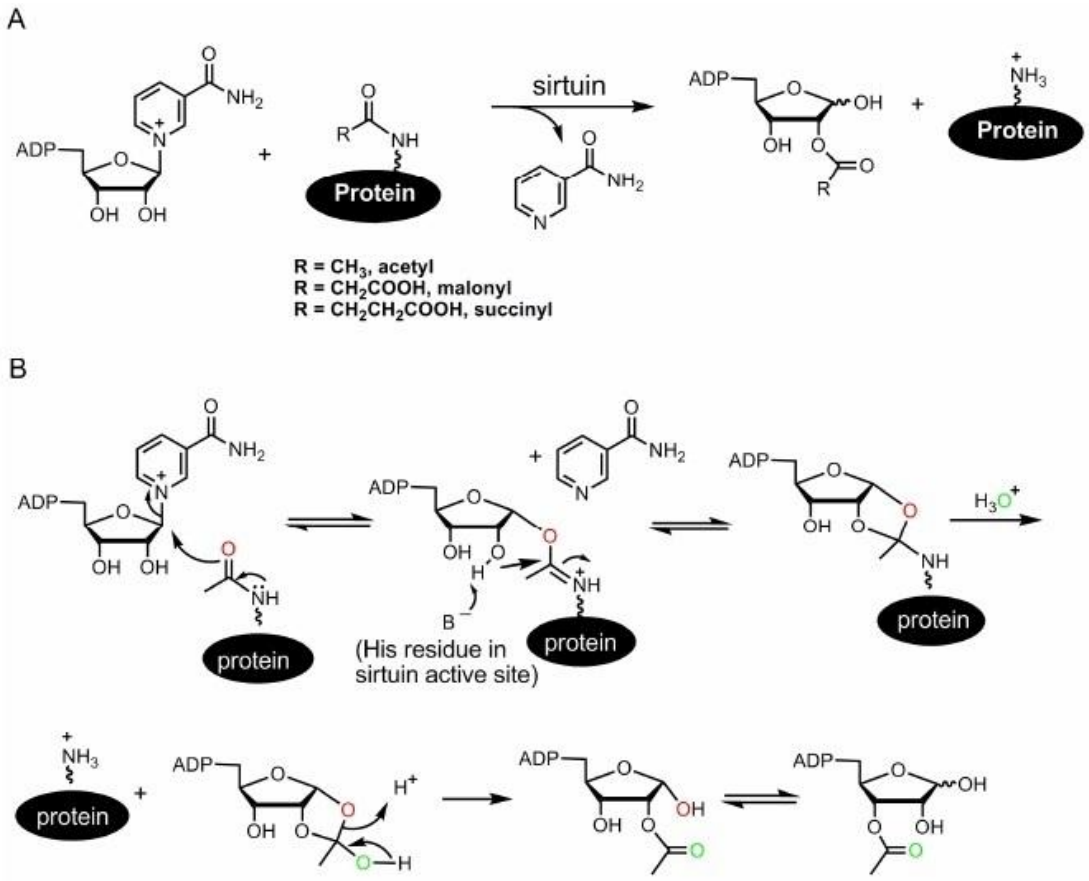

Fig. 2.1 (**A**) The sirtuins catalyzed NAD-dependent deacylation reaction is shown, and the reaction generates *O*-acyl-ADP-ribose. (**B**) Mechanism of sirtuin catalyzed NAD-dependent deacetylation. Some of the oxygen atoms are colored differently to indicate where they come from.

contrast with other sirtuins (Sirt1, HST2), which possess robust deacetylation activity but show little preference for peptide sequences. I showed that human Sirt6 could accommodate sequences other than H3K9 and efficiently remove the myristoyl group from sequences like H2BK12 and H4K16. No hydrolysis by Sirt6 has been previously reported for the acetyl modified version of these peptides. Further, in collaboration with Wang *et al.*, we crystallized Sirt6 with H3K9myr peptide. The crystal structure unveils a large hydrophobic pocket that can accommodate the long chain fattyacyl groups. This

further supported our enzymology data. Since Sirt6 has been known to be a nuclear protein and has been associated with histones, I also wanted to explore whether histones might have fattyacyl modifications as an epigenetic mark. In the results section, I present some of the key experiments that I performed towards that end.

Later, my colleague Hong Jiang extended this work and showed that Sirt6 promotes the secretion of TNFα by removing the fattyacyl modification on Lys19 and Lys20 of TNFα. Protein lysine fattyacylation has been known to occur in mammalian cells (31, 32) on the TNFα protein, but the regulatory mechanism of this modification was unknown. Together, our data suggest that protein lysine fattyacylation is a novel mechanism for regulating protein secretion. The discovery of Sirt6 as an enzyme that controls protein lysine fattyacylation provides new opportunities to investigate the physiological function of these previously less known PTMs.

2.3 Methods and Materials

Cloning, Expression, and Purification of Full Length Sirt6 for Activity Assay

The open reading frame of full length human Sirt6 (1-355) was inserted into a pET28a vector between the BamHI and NotI sites. This plasmid was transformed in the *E. coli* ArcticExpress (DE3) cells. The cells were cultured at 37 °C in 2×YT culture medium (5 g of NaCl, 16 g of bactotrypton, and 10 g of yeast extract per liter). To induce the protein expression, isopropyl-β-D-1-thiogalactopyranoside (IPTG) was added to a final concentration of 0.2 mM and when OD_{600} was 0.6-0.8, the culture was grown for another 48 h at 12 °C. Cells were harvested by centrifugation at 7,330 g for 10 min at 4

°C and then re-suspended in lysis buffer (20 mM Tris-HCl, pH 7.2, 500 mM NaCl and 2% glycerol). The suspension was lysed using Avestin emulsiflex cell disrupter and then centrifuged at 29,300 g for 25 min at 4 °C. The supernatant was loaded onto a nickel column (QFF-sepharose, Amersham Biosciences, Sweden) pre-equilibrated with a buffer containing 20 mM Tris-HCl, pH 7.2, 500 mM NaCl. The target protein was eluted with a linear gradient of 0 to 500 mM of imidazole freshly prepared in the lysis buffer. The desired fractions were pooled, concentrated, and buffer exchanged against the cation exchange buffer (80 mM NaCl, 20 mM Tris-HCl, pH 7.2, 5% glycerol). The protein was then loaded onto a cation exchange column (Amersham Biosciences, Sweden) and was eluted with 1 M NaCl, 20 mM Tris-HCl, pH 7.2, 2% glycerol. Fractions were assayed for purity on SDS-PAGE gel, and the desired fractions were concentrated and stored at -80 °C for later use.

Activity Assay using LC-MS

The activity of Sirt6 was determined using HPLC to separate the reaction mixture by detecting the modified and unmodified WWH3K9 peptides using a mass spectrometer coupled to it. The reaction comprised of 20 mM of Tris pH 8.0, 1 mM DTT, 50 µM WWH3K9 modified peptide, 0.5 mM of NAD and 2.8 µM of Sirt6 (truncated or full length) in a 60 µL reaction volume and was incubated at 37 ^{o}C for 1 h. The reaction was stopped with 1 volume of 0.5 N HCl in methanol (methanol was used to ensure the solubility of hydrophobic fattyacyl peptide) and spun down for 10 min at 18,000 g (Beckman Coulter Microfuge) to separate the protein from the reaction mixture. The supernatant was then analyzed by LC-MS on a SHIMADZU LC-MS-QP8000α with a

Sprite TARGA C18 column (40 × 2.1 mm, 5 μM, Higgins Analytical, Inc., Mountain View, CA). The LC was monitored at 215 and 280 nm. Solvents used in LC-MS were water with 0.1% formic acid and acetonitrile with 0.1% formic acid.

Kinetic Assay for Acetyl and Butyryl Peptides

The acetyl or butyryl peptides were dissolved in 25% DMSO water mixture. The concentrations of peptides were determined at 280 nm using extinction coefficient of the two tryptophan residues attached at the C-terminus of the peptides (since the tryptophan residues added to the peptides absorb predominantly at this wavelength). The final DMSO concentration in the reaction mixture was maintained at 2.5%. Peptide concentrations were varied from 0 to 250 μM for H3K9 butyryl peptide and from 0 to 600 μM for the acetyl peptide. The reactions containing 2 mM NAD, 1 mM DTT, 20 mM Tris, pH 8.0, 4 μM recombinant Sirt6 full length, and acyl peptides at various concentrations were incubated for 30 min at 37 °C. The reactions were stopped using 1 volume of 0.5 N HCl in methanol. The reaction mixtures were spun at 18,000 g for 10 min and were analyzed on a Kinetex XB-C18 column (100 Å, 100 mm × 4.60 mm, 2.6 μm, Phenomenex). The gradient of 20-40% B in 17 min at 0.5 mL/min was used. The product peak and the substrate peak were quantified using absorbance at 280 nm and converted to initial rates. Initial rates were then plotted against the acyl peptide concentration and fitted using the software KaleidaGraph.

Kinetic Assay for Long Chain Fattyacyl Peptides

The longer chain fattyacyl peptides were dissolved in pure DMSO. The concentrations of peptides were determined at 280 nm using extinction coefficient of the two tryptophan residues attached to the C terminus of the peptides (since the tryptophan residues added to the peptides absorb predominantly at this wavelength). The final DMSO concentration in the reaction mixture was maintained at 2.5%. The peptide concentrations were varied from 1 to 20 µM. The reactions containing 2 mM NAD, 1 mM DTT, 20 mM Tris pH 8.0, 0.2 µM recombinant Sirt6 full length, and acyl peptides at different concentrations were incubated for 15 min at 37 °C. The reactions were stopped using 1 volume of 0.5 N HCl in methanol. The reaction mixtures were spun at 18,000 g for 10 min and were analyzed on Kinetex XB-C18 column (100 Å, 75 mm × 4.60 mm, 2.6 µm, Phenomenex). The gradient of 0-55% B in 10 min at 0.5 ml//min was used. The product peak and the substrate peak were quantified using absorbance at 280 nm and converted to initial rates. Initial rates were then plotted against the acyl peptide concentration and fitted using the software KaleidaGraph.

Isolation of 2´-O Myristoyl ADP-ribose

The reaction was carried out as described previously in the activity assay except that instead of 1 mM NAD, we used 0.25 mM NAD and 4 µM recombinant Sirt6 (1-314). The reaction was quenched using 10% TFA in 90% acetonitrile. The quenching solution was critical due to the hydrophobic nature and stability of the 2´-O-myristoyl ADP-ribose. The reaction was analyzed on reverse phase HPLC using C18 Vydac column (250 × 4.6 mm, 90 Å, 10 µM, Grace Vydac, Southborogh, MA). A gradient of 0-40% B in 15 min,

10%-100% B in 15 min was used to separate the intermediate from the reaction mixture. The buffer A was water and 0.1% TFA and buffer B was 100% acetonitrile in 0.1% TFA. The myristoyl ADP-ribose was collected, lyophilized, and redissolved in 50% acetonitrile water and submitted for MALDI–TOF mass spectroscopy in the negative mode.

^{32}P-NAD Radiolabeling Assay

Different peptides (50 μM) were incubated with 2 mM DTT and 50 mM Tris pH 8.0, 500 mM NaCl buffer, 1 μM Sirt6 and 0.1 μCi ^{32}P-NAD (purchased from American Radiolabeled Chemicals Inc.) in a 10 μL reaction tube at 37^{o}C for 2 h. Then, 1 μL of reactions mixture was spotted on a plastic backed silica gel TLC plate. The solvent system consisting of 70% ethanol and 30% 2.5 M ammonium acetate was used to resolve the reaction mixture. The ^{32}P-NAD and products were detected by autoradiography.

Digestion of Histone

For trypsin digestion of calf thymus histone, 2 mg of the protein was dissolved in 6 M urea, 60 mM Tris-HCl (pH 8.0), 15 mM DTT in a 250 μL reaction volume. The solution was heated at 37 °C for 30 min and then cooled to room temperature. Then, 22.5 μL of 1 M iodoacetamide was added in order to achieve a final concentration of approximately 50 mM. The reaction mixture was incubated at room temperature with gentle mixing for 1 h in a dark tube. Then, 3.6 mL of 50 mM Tris-HCl (pH 7.4) with 1 mM $CaCl_2$ was added to the reaction mixture to lower the urea concentration to 0.75 M.

For the digestion step, 150 μL of 100μg/mL modified and activated trypsin (Promega Corporation, Madison, WI) was added and the reaction mixture was incubated

at 37 °C for 12-16 h. The reaction was quenched by adding 120 µL 10% TFA and the pH was adjusted to 2~3. The digested peptides were desalted by using Sep-Pak C18 cartridge 1 cc/50 mg (Waters Corporation, Milford, MA) and lyophilized in glass vials. All the steps were performed as per the instructions on the cartridge. However, the elution step was modified in which instead of the usual 50% acetonitrile-water, another elution was performed with 90% acetontrile-water to ensure the elution of the hydrophobic peptides. The eluted peptides were lyophilized in glass vials and dissolved in minimum amount of water or dimethylsulfoxide.

Peptide Synthesis

The WWH3K9 (NH2-KQTARK*STGGWW-COOH) backbone was prepared using standard solid phase peptide synthesis (SPPS) at room temperature (RT). Briefly, 100 mg Wang resin SS (100-200 mesh, 1% DVB, 10 mMole/g) was swollen in a peptide synthesis vessel with 5 ml of anhydrous dichloromethane (DCM) for 5 h. After draining off the solvent, resin was washed with 5 ml *N*, *N*-dimethylformamide (DMF). The reaction mixture containing the first amino acid namely Fmoc-tryptophan-OH (0.32 millimoles, 3 equivalents) along with O-benzotriazole-*N*, *N*, *N´*, *N´*-tetramethyl-uranium-hexafluoro-phosphate (HBTU, 0.133 millimoles, 1 equivalent) and 4-dimethylaminopyridine (DMAP) was dissolved fully in 5 ml of anhydrous DMF. To this, 0.64 millimoles of diisopropylethylamine (DIEA) were added as base and the reaction mixture solution was then added to the resin. The resin was incubated with the solution overnight at RT. The resin was washed with 5 ml DMF for 5 times. The excess reactive functionalities on the resin were blocked using a solution of acetic acid, pyridine, and

DMF in 2:1:3 ratios, respectively for 30 min. After draining off the blocking solution, the resin was washed and Kaiser test reference was used to test the success of the coupling. Once coupling was confirmed, the resin was treated with a 20% piperidine in DMF solution for 5 min to remove the Fmoc group. The treatment with piperidine was repeated for 20 min for the second time with a fresh batch of piperidine in DMF solution in order to ensure a full deprotection. The resin was washed three times with DMF, and then again three times with DCM, a Kaiser test was performed at this point to ensure that the deprotection worked. Finally, the resin was washed three times with DMF before adding the next amino acid again. All subsequent activated amino acid derivatives were freshly prepared by dissolving 0.24 millimoles of the amino acid, 0.24 millimoles of HBTU, and 0.21 millimoles of N-hydroxybenzotriazole (HOBT) in 5 ml of DMF. Lastly, 0.48 millimoles of DIEA was added to above mixture and the resulting solution was in turn added to the resin. The suspension was incubated for at least 2 h at RT.

The lysine to be modified by different acyl groups (K*) was protected with Alloc on the side chain while the N-terminal lysine was protected by Boc at both the side chain and at the amino group terminus. After the addition of all the amino acids, the Alloc group was removed using a solution of DCM, morpholine (Sigma, 2.5% v/v), and glacial acetic acid (5% v/v) with a 1:1 (w:w) ratio of the original resin and tetrakis (triphenylphosphine) palladium(0) for 4 h under nitrogen at RT. The resin was washed with 0.5% DIEA in DCM for 5 min and the washing was repeated five times. The resin was again washed at least two times with 0.02 M of diethyldicarbamate in DMF, each time for 30 min to remove the palladium. The resin was subjected to the acylation solutions containing 0.24 mMoles fatty acid of different chain lengths (acetic anhydride,

butyric acid, octanoic acid, myristic acid, dodecanoic acid, palmitic acid etc.), 0.24 mMole of HBTU, 0.21 mMole of HOBT, 0.48 mMole of DIEA, and anhydrous DMF overnight at RT. The resin was then washed with DMF and DCM in that order. To cleave the peptide from the resin, the dried resin was subjected to a concoction of TFA, 5% water, 5% phenol, 2.5% ethanedithiol, and 5% thioanisole for 2-4 h at RT. The solution containing the cleaved peptide was filtered and the TFA was removed by flushing N2 gas or air over the filtrate. The peptide was precipitated by adding ether three times. Ether was then removed by decantation and the crude peptide was lyophilized. The crude peptide was dissolved in water containing 1% TFA, was subjected to HPLC (Beckman Coulter System Gold 125P solvent module and 168 Detector) separation. The HPLC separation was done on TARGA C18 column (250 x 20 mm, 10 μM, Higgins Analytical, Inc., Mountain View, CA) with mobile phase A (water with 0.1% TFA) and B (acetonitrile with 0.1% TFA) at a gradient of 20% B to 100% B in 50 min and a flow rate of 10 mL/min. The peptide was monitored at both 215 nm and 254 nm, and the fractions were collected. LC-MS (SHIMADZU LC-MS-QP8000α with a Sprite TARGA C18 column (40 × 2.1 mm, 5 m, Higgins Analytical, Inc., Mountain View, CA) was used to confirm the peptide mass and the high purity fractions were lyophilized. For the LC-MS runs, the peptide could be observed at both 215 nm and 280 nm, and the solvents used were water with 0.1% formic acid and acetonitrile with 0.1% formic acid. Purified peptide was either dissolved in water or in DMF and the concentration was determined using UV spectroscopy. Other peptides were synthesized similarly as described above.

2.4 Results

Sirt6 was first expressed in *Escherichia coli* Rosetta (*E. Coli* BL21R2-DE3) cells. However, since the full length protein was not stable, very little soluble protein was obtained from these cells. The truncated form of Sirt6, Sirt6 (1-314), with the conserved core catalytic domain still intact was expressed. The truncated protein was obtained using Ni-resin purification followed by gel-filtration purification as shown in Fig. 2.2.

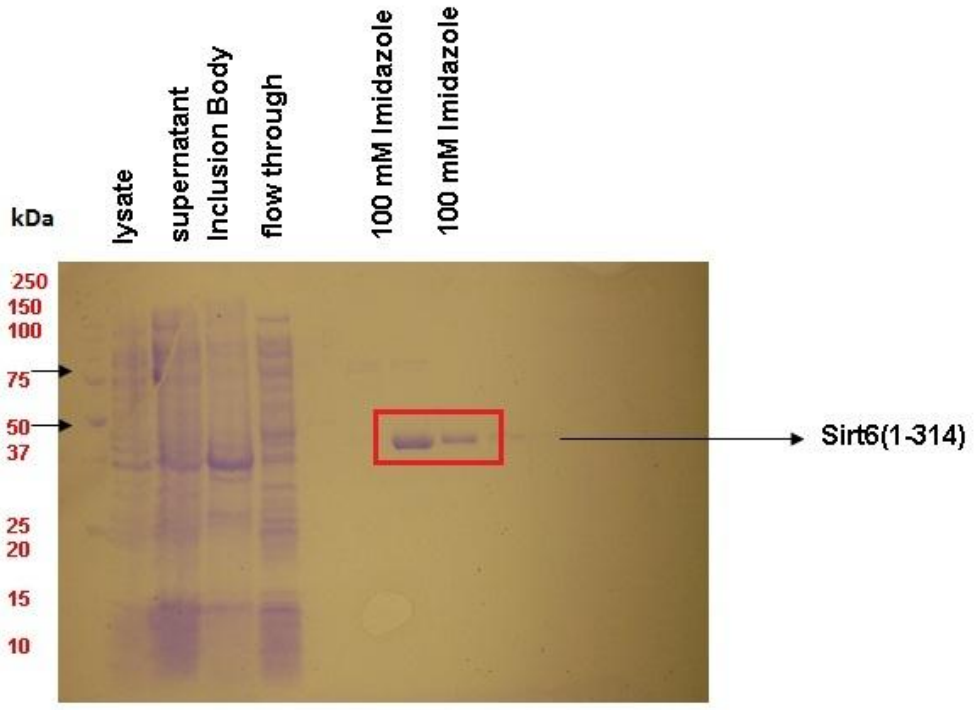

Fig. 2.2 Ni – NTA affinity purification of human Sirt6 (1-314) in *E. coli* BL21R2 cells; the expected molecular weight is 39 kDa.

Sirt6 has been previously known to be sequence specific in its deacetylase activity for H3K9 and H3K56 histone peptides (19, 20, and 27). We therefore chose the H3K9 peptide as our model for the peptide backbone with K9 being the site for different physiologically relevant modifications, namely acetylation, propionylation, butyrylation, biotinylation, lipoylation, glutrylation, SUMOylation, and ubiquitylation. The

SUMOylation and ubiquitylation meant small peptide sequences (i.e. for SUMO1 NH_2DVIEVYQEQTGG and for NEDD8 NH_2LHLVLALRGG) from the SUMO and ubiquitin proteins as the 'acyl' modifications on K9 of the H3K9 peptide. A small peptide library, as shown in Fig. 2.3, was generated using the synthesis scheme as described in the literature (33). The synthesized peptides were subjected to reverse phase HPLC purification. Identity of the peptides was confirmed using mass spectroscopy. Table 2.1 presents the sequences, and the observed and expected masses of the synthesized peptides.

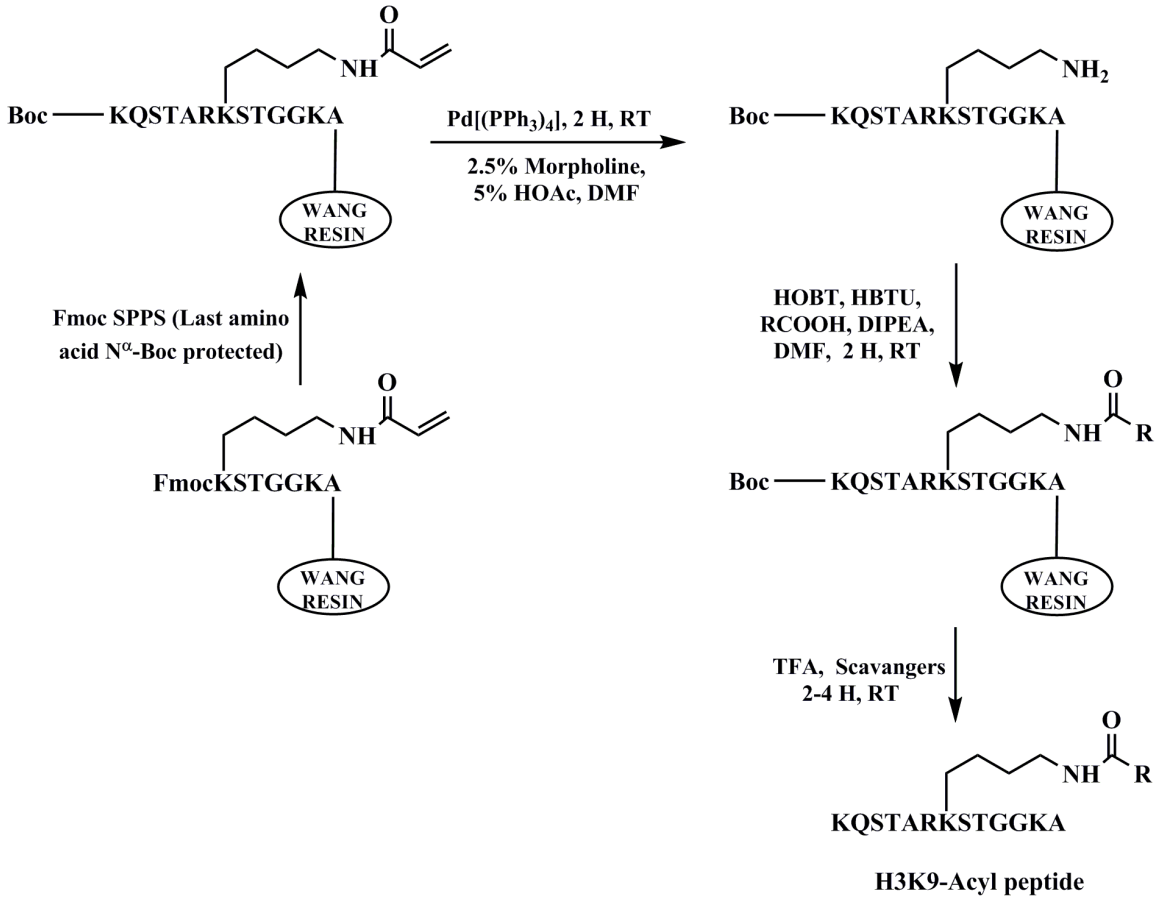

Fig. 2.3a Synthesis scheme for making the 'acyl' peptide library on the lysine 9 of the histone H3K9 peptide sequence.

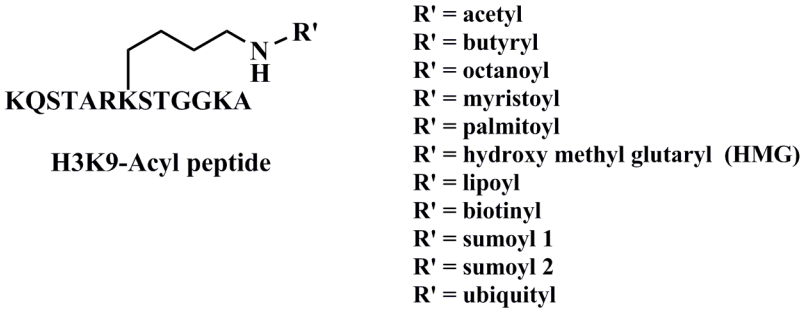

Fig. 2.3b Various peptides made using the scheme as described above.

Table 2.1 List of peptides synthesized their sequences, observed and expected masses

Peptide	Observed Mass	Expected Mass	Peptide Sequence
H3K9Acetyl	1274.0	1273.71	KQTAR(AcK)STGGKA
H3K9Propionyl	1287.8	1288.73	KQTAR(ProK)STGGKA
H3K9Lipoyl	1422.15	1419.73	KQTAR(LipK)STGGKA
H3K9Biotin	1457.85	1457.78	KQTAR(BiotinK)STGGKA
H3K9Transoctenoic Acid	1355.75	1355.79	KQTAR(OctenoicK)STGGKA
H3K9Myristoyl	1441.95	1441.9	KQTAR(MyrK)STGGKA
H3K9Palmitoyl	1470.25	1469.93	KQTAR(PalmK)STGGKA
H3K9HMG	1375.2	1375.74	KQTAR(HMGK)STGGKA HMG -Hydroxymethyl glutarate
H3K9SUMO1	1387.20	2772.37	*KQTAR(SUMO1K)STGGKA SUMO-1:DVIEVYQEQTGG *K is Fmoc protected
H3K9SUMO2	1264.7	2527.28	*KQTAR(SUMO2K)STGGKA SUMO-2: IDVFQQQTGG *K is Fmoc protected
H3K9NEDD8	1800.072	1799.049	KQTAR(NEDD8K)STGGKA NEDD8: LHLVLA
H2BK12Acetyl	1831.05	1832.05	PEPAKSAPAPKK(Ac)GSKKWW
H2BK12Myristoyl	2000.05	2000.24	PEPAKSAPAPKK(Myr)GSKKWW
H3K9Acetyl	1447.67	1446.74	KQTAR(AcK)STGGWW
H3K9Butyryl	1475.42	1474.77	KQTAR(ButK)STGGWW
H3K9Octanoyl	1532.67	1530.83	KQTAR(OctK)STGGWW
H3K9myristoyl	1616.5	1614.9	KQTAR(MyrK)STGGWW

The activity of the recombinant Sirt6 (1-314) on these different acyl peptides was assessed by using a high-performance liquid chromatography (HPLC) based *in vitro* assay coupled to a mass spectrometer (details of the activity assay are described in Section 2.3). The truncated Sirt6 (1-314) was indeed found to deacylate comparatively longer chain fattyacyl groups such as palmitoyl, myristoyl, and lipoyl peptides better than the acetyl, succinyl, glutaryl, and ubiquitylated H3K9 peptides (Table 2.1). The following figures show the LC-MS traces of the activity assay for some of the acyl peptides. The vertical axis in the figures shows the ion intensities (10 × magnified) and the horizontal axis show the retention time of the acylated and deacylated peptides. The mass of the acylated peptides are shown in Table 2.1 and that of the deacylated peptide is 1232.0. The activity for different peptides was detected by the presence of deacylated peptide mass intensities, which are shown as pink traces in the figures.

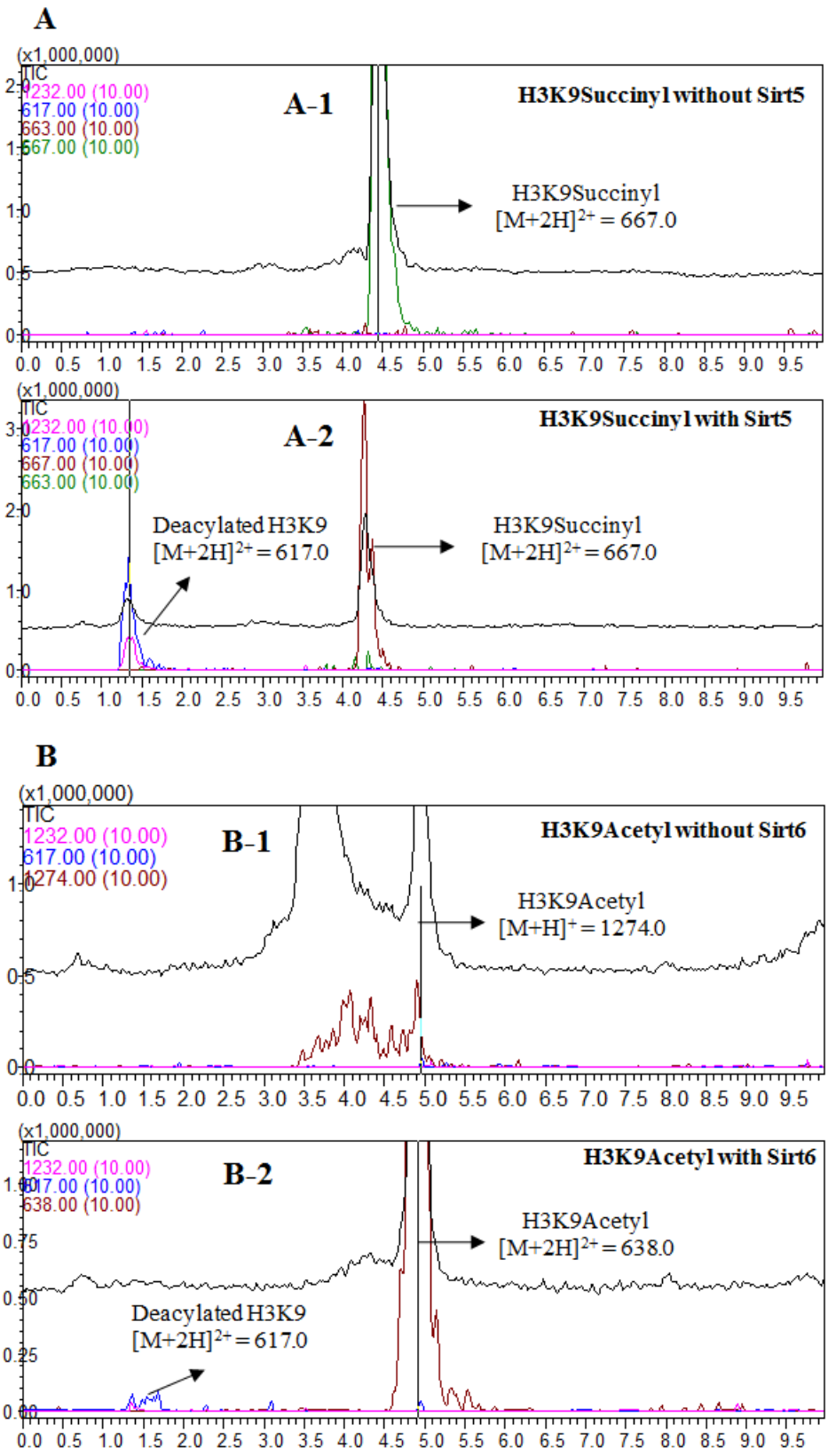
A
(x1,000,000)
TIC
1232.00 (10.00)
617.00 (10.00)
663.00 (10.00)
667.00 (10.00)
A-1
H3K9Succinyl without Sirt5
H3K9Succinyl
[M+2H]2+ = 667.0
(x1,000,000)
TIC
1232.00 (10.00)
617.00 (10.00)
667.00 (10.00)
663.00 (10.00)
A-2
H3K9Succinyl with Sirt5
Deacylated H3K9
[M+2H]2+ = 617.0
H3K9Succinyl
[M+2H]2+ = 667.0
B
(x1,000,000)
TIC
1232.00 (10.00)
617.00 (10.00)
1274.00 (10.00)
B-1
H3K9Acetyl without Sirt6
H3K9Acetyl
[M+H]+ = 1274.0
(x1,000,000)
TIC
1232.00 (10.00)
617.00 (10.00)
638.00 (10.00)
B-2
H3K9Acetyl with Sirt6
H3K9Acetyl
[M+2H]2+ = 638.0
Deacylated H3K9
[M+2H]2+ = 617.0

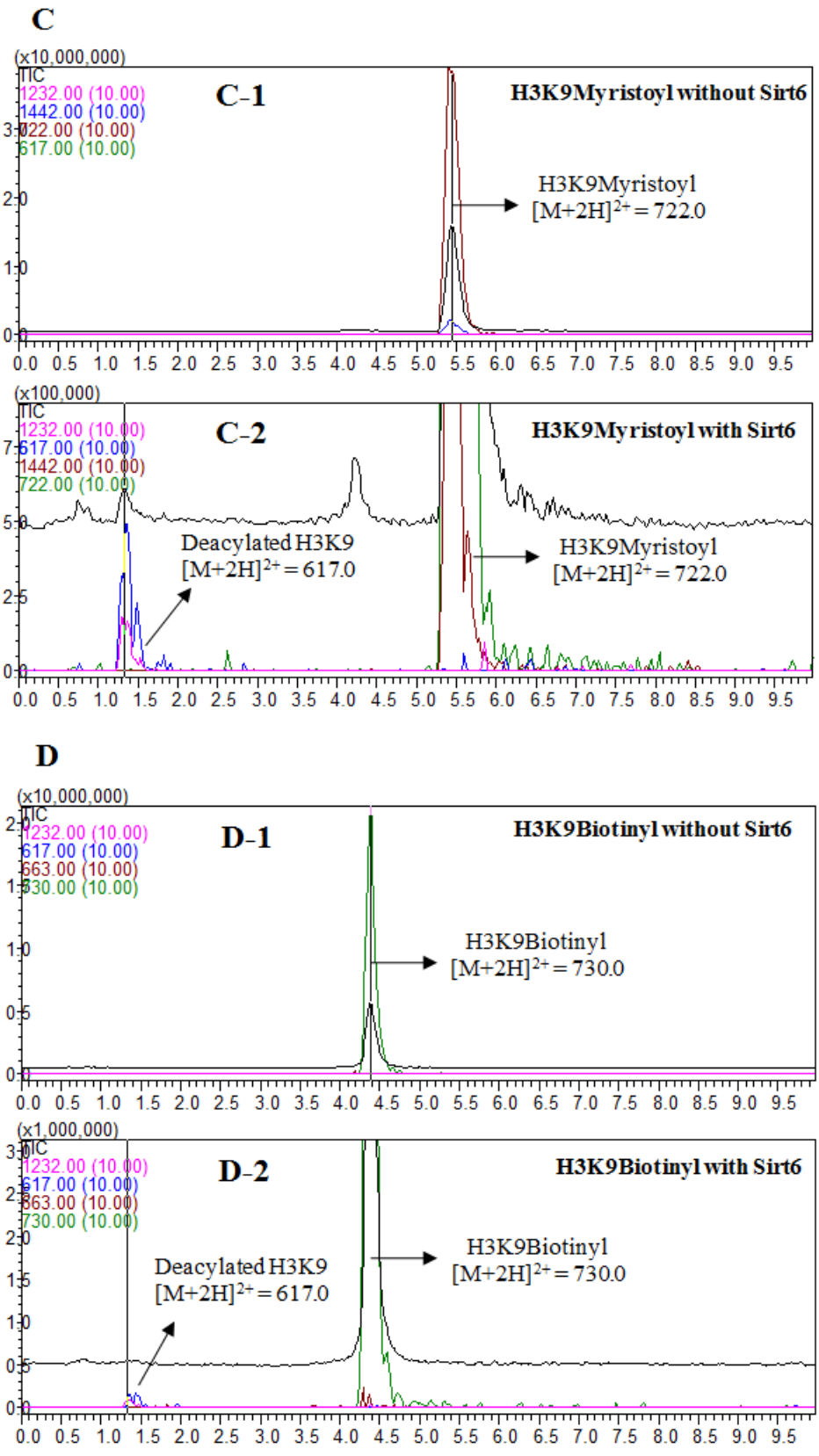
C
(x10,000,000)
TIC
1232.00 (10.00)
1442.00 (10.00)
722.00 (10.00)
617.00 (10.00)
C-1
H3K9Myristoyl without Sirt6
H3K9Myristoyl
[M+2H]2+ = 722.0
(x100,000)
TIC
1232.00 (10.00)
617.00 (10.00)
1442.00 (10.00)
722.00 (10.00)
C-2
H3K9Myristoyl with Sirt6
Deacylated H3K9
[M+2H]2+ = 617.0
H3K9Myristoyl
[M+2H]2+ = 722.0
D
(x10,000,000)
TIC
1232.00 (10.00)
617.00 (10.00)
663.00 (10.00)
730.00 (10.00)
D-1
H3K9Biotinyl without Sirt6
H3K9Biotinyl
[M+2H]2+ = 730.0
(x1,000,000)
TIC
1232.00 (10.00)
617.00 (10.00)
663.00 (10.00)
730.00 (10.00)
D-2
H3K9Biotinyl with Sirt6
Deacylated H3K9
[M+2H]2+ = 617.0
H3K9Biotinyl
[M+2H]2+ = 730.0

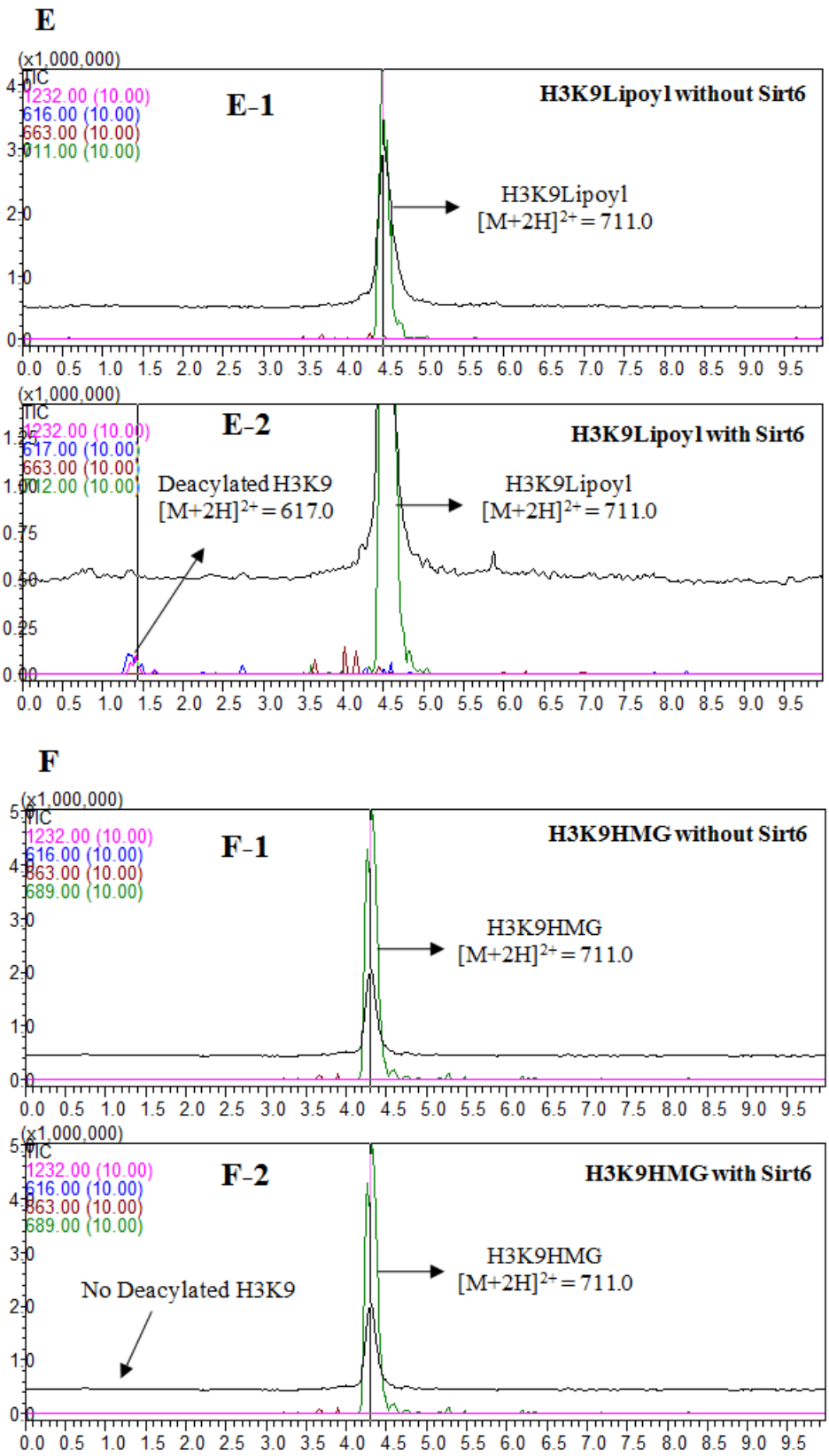
E
(x1,000,000)
TIC
1232.00 (10.00)
616.00 (10.00)
663.00 (10.00)
711.00 (10.00)
E-1
H3K9Lipoyl without Sirt6
H3K9Lipoyl
[M+2H]2+ = 711.0
(x1,000,000)
TIC
1232.00 (10.00)
617.00 (10.00)
663.00 (10.00)
712.00 (10.00)
E-2
H3K9Lipoyl with Sirt6
Deacylated H3K9
[M+2H]2+ = 617.0
H3K9Lipoyl
[M+2H]2+ = 711.0
F
(x1,000,000)
TIC
1232.00 (10.00)
616.00 (10.00)
663.00 (10.00)
689.00 (10.00)
F-1
H3K9HMG without Sirt6
H3K9HMG
[M+2H]2+ = 711.0
(x1,000,000)
TIC
1232.00 (10.00)
616.00 (10.00)
663.00 (10.00)
689.00 (10.00)
F-2
H3K9HMG with Sirt6
No Deacylated H3K9
H3K9HMG
[M+2H]2+ = 711.0

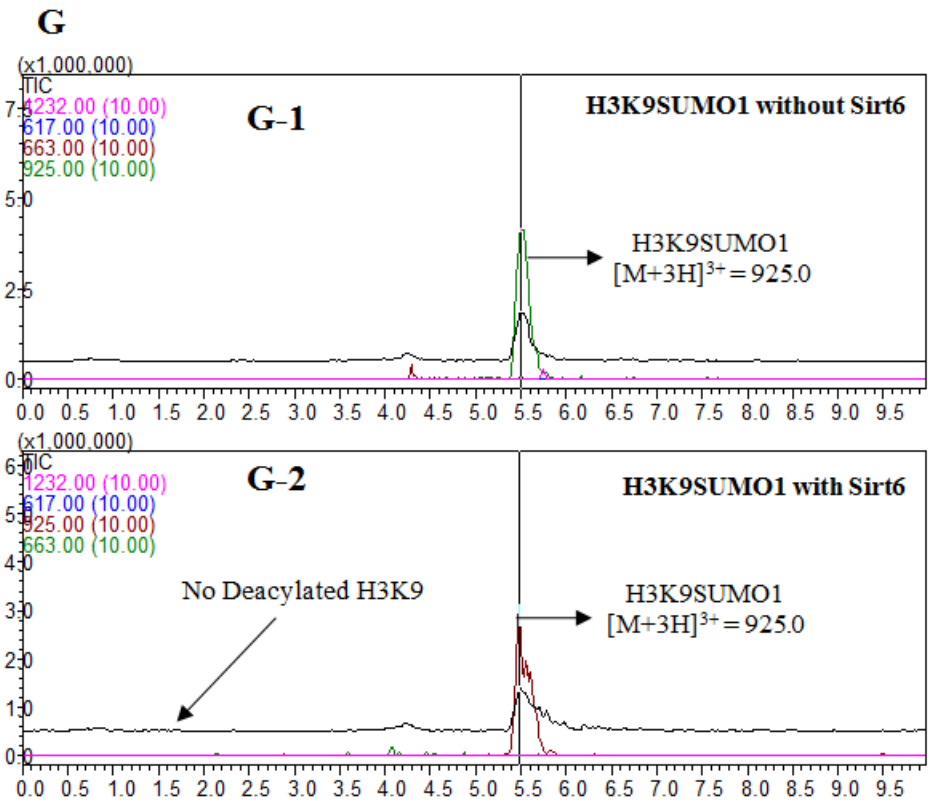

Fig. 2.4 Sirt6 (1-314) catalyzes the hydrolysis of myristoyl lysine on the histone H3K9 based sequence. Sirt6 and Sirt5 catalyzed reactions were analyzed by LC-MS, with Sirt5 being the positive control for desuccinylation (Fig. 2.4A). For each reaction, the MS trace (Fig. 2.4A-2.4G) shows the ion intensities (10 × magnified) for the acylated peptides and the deacylated peptides.

To facilitate the UV detection of the peptides, two tryptophan residues were added to C terminus of the H3K9 backbone peptide. This enabled the detection of peptides in the kinetic assay as described in Section 2.3. The H3K9 and WWH3K9 peptides were used interchangeably in all assays and the choice has been marked clearly in all figures described in this thesis.

In order to further confirm the results from the activity assays described above, a ^{32}P-NAD-based biochemical assay was used. Based on the known deacylation mechanism of sirtuins (Fig. 2.1 B), the demyristoylation of the fattyacyl H3K9 peptide by Sirt6

should generate 2´-O-myristoyl ADP-ribose. When incubating myristoyl H3K9 with Sirt6 (1-314) and ^{32}P-NAD, most of the NAD was consumed and a new very less polar spot that ran almost at the solvent front was observed (Fig. 2.5). This is consistent with the formation of 2´-O-myristoyl ADP-ribose, since the hydrophobic myristoyl will make the intermediate acyl-ADP-ribose less polar. When acetyl H3K9 peptide was incubated with Sirt6 (1-314) and ^{32}P-NAD, although a new product (2´-O-acetyl ADP-ribose) spot was observed, there were still NAD molecules left. The data suggested that Sirt6 catalyzed demyristoylation is more efficient than deacetylation.

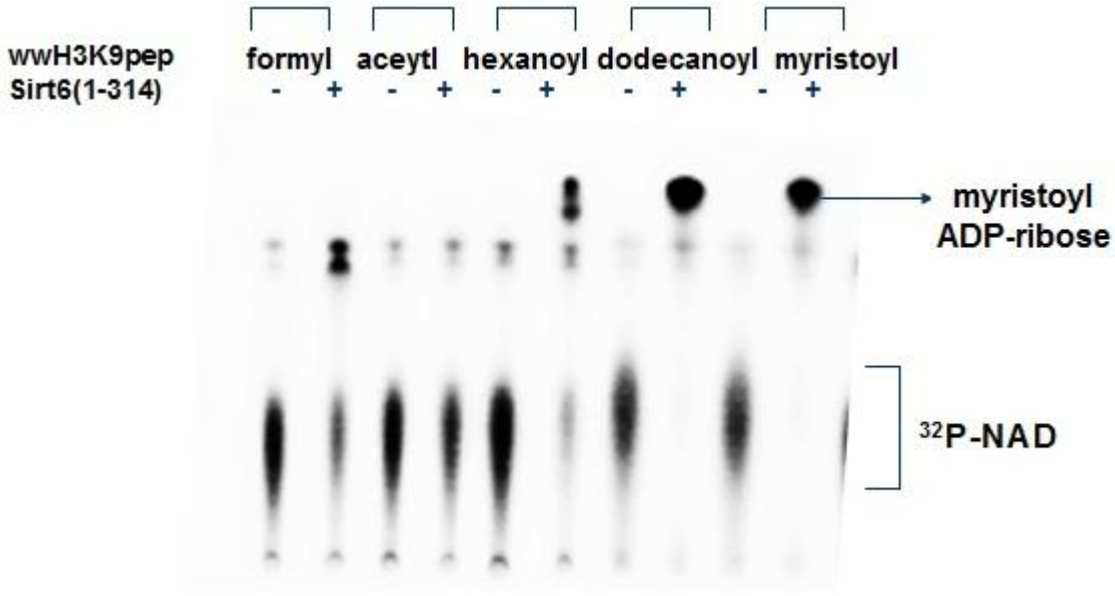

Fig. 2.5 Biochemical ^{32}P-NAD assay of the Sirt6 (1-314) with various H3K9acyl peptides, which shows the formation of less polar 2´-O-fattyacyl-ADP-ribose.

We also confirmed the formation of the 2´-O-myristoyl-ADP-ribose obtained from the *in vitro* assay using MALDI – TOF mass spectroscopy (Fig. 2.6a-c). Firstly, the reaction intermediate was isolated. Two main challenges of isolating this reaction product

were its stability and solubility in our acidic quenching solution (0.5 N HCl in methanol). To isolate the 2´-O-myristoyl-ADP-ribose intermediate, we switched to a milder quenching solution of 10% TFA in 90% acetonitrile-water. The intermediate was isolated by separating the reaction mixture using reverse phase HPLC (Fig. 2.6a). The isolated intermediate was lyophilized and subjected to MALDI-TOF mass spectrometry in the negative mode. The presence of O-myristoyl-ADP-ribose was verified by the presence of a mass peak of 768.31 (Fig. 2.6b). This was absent in the negative control (Fig. 2.6c).

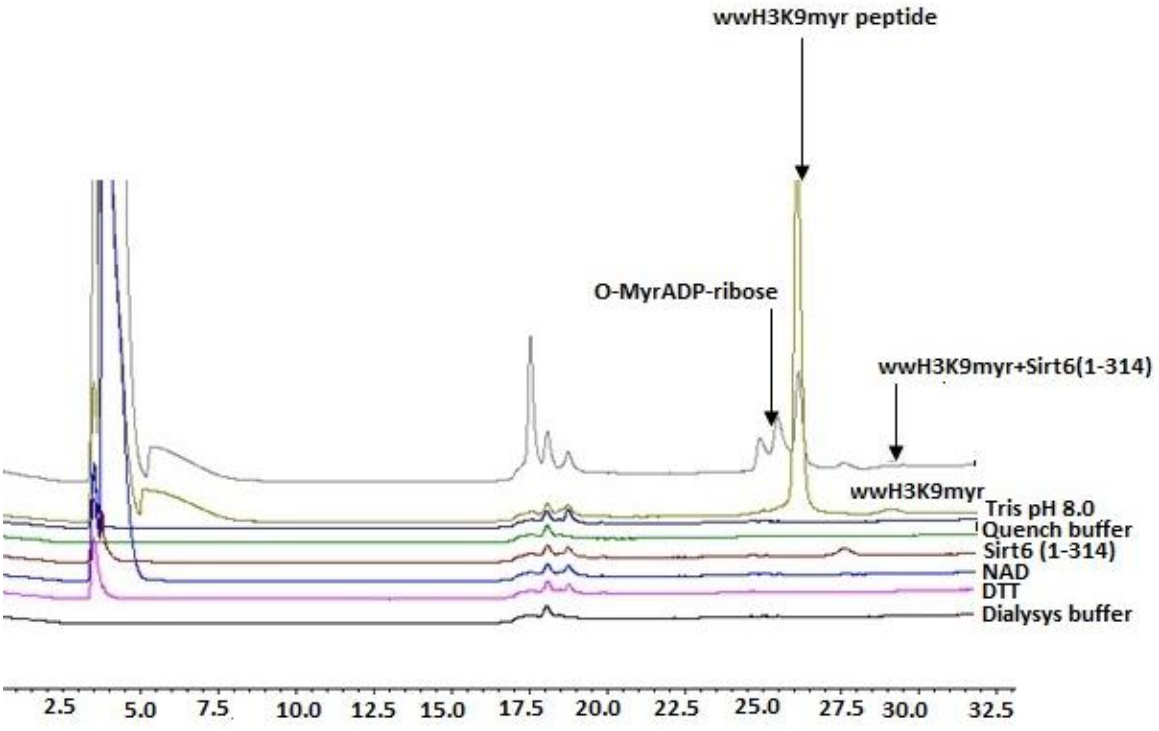

Fig. 2.6a HPLC trace for the separation of 2´-O-myristoyl-ADP-ribose from the reaction mixture.

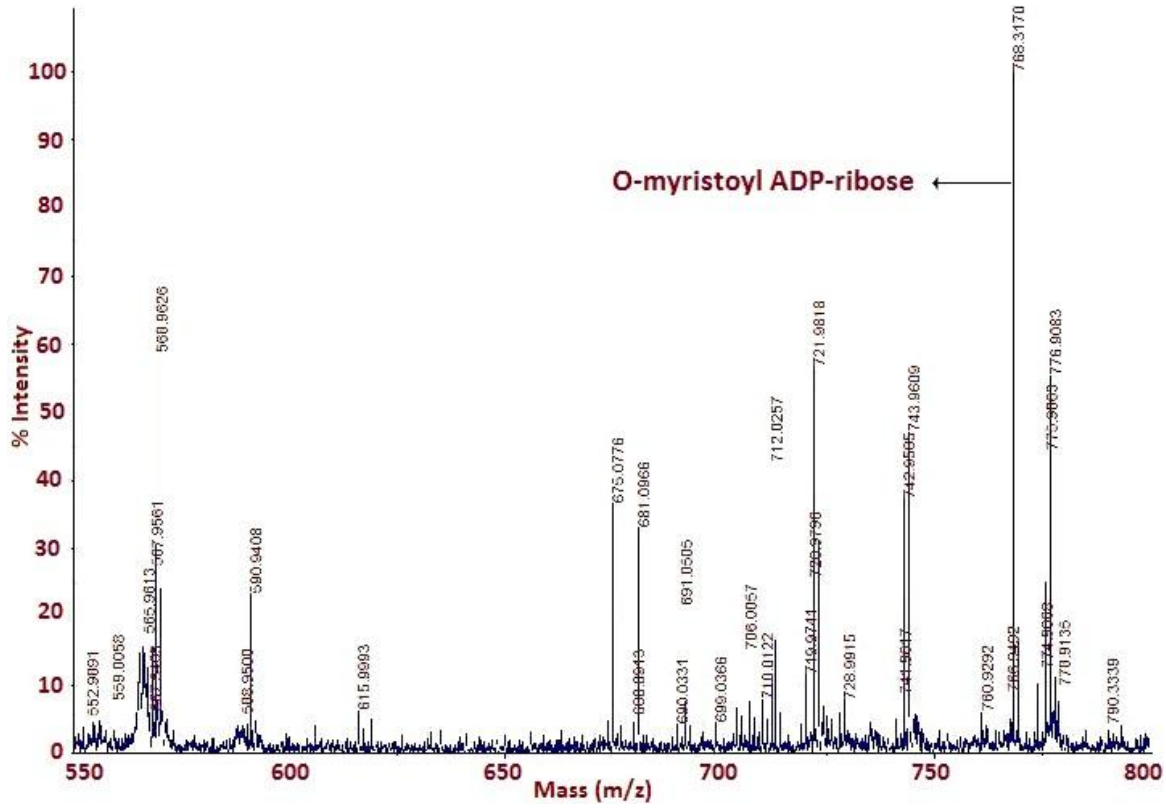

Fig. 2.6b MALDI-TOF spectra for the O-myristoyl-ADP-ribose peak collected from the positive control (reaction mixture with Sirt6) shows the presence of desired mass peak with m/z of 768.31.

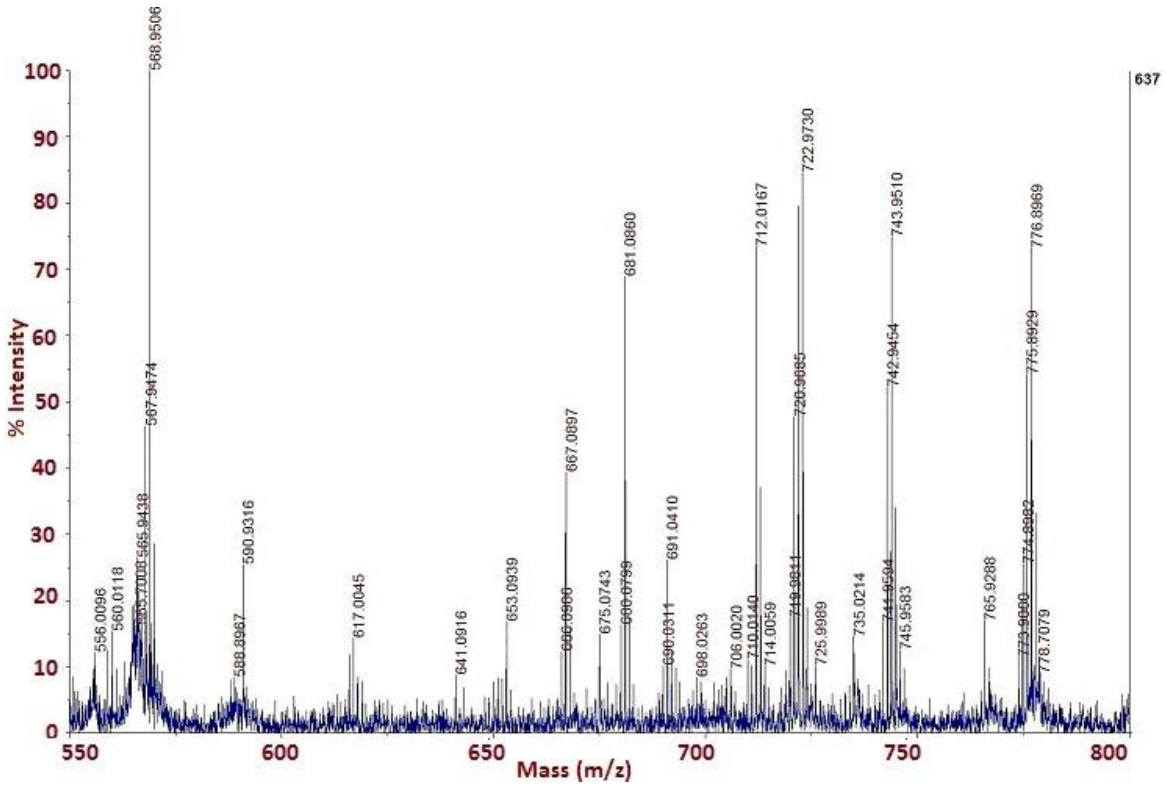

Fig. 2.6c MALDI-TOF spectra for the O-myristoyl-ADP-ribose peak collected from the negative control (reaction mixture without Sirt6) shows no mass peak corresponding with m/z of 768.31.

After determining the more efficient activity for Sirt6, I tested whether the new defattyacylation activity would allow Sirt6 to accept other peptide sequences as substrates as is the case with other sirtuins (Sirt1-3), which are known to have a strong deacetylation activity but no specificity. For this purpose, I synthesized acetyl and myristoyl peptides based on H2BK12 and H4K16 histone sequences (Table 2.1). Consistent with the earlier report (20), the hydrolysis of these acetyl peptides by Sirt6 was essentially undetectable based on the HPLC analysis. In contrast, the hydrolysis of the corresponding myristoyl peptides can be readily detected (Fig. 2.7). This activity was also confirmed by detecting the mass of the hydrolyzed or deacylated peptide using HPLC analysis coupled with mass

spectroscopy or LC-MS assay (data not shown). These results further support that the defattyacylase activity of Sirt6 is more efficient than its deacetylase activity. We hence concluded that with the appropriate acyl group, Sirt6 can catalyze the hydrolysis of acyl lysine on different peptide sequences.

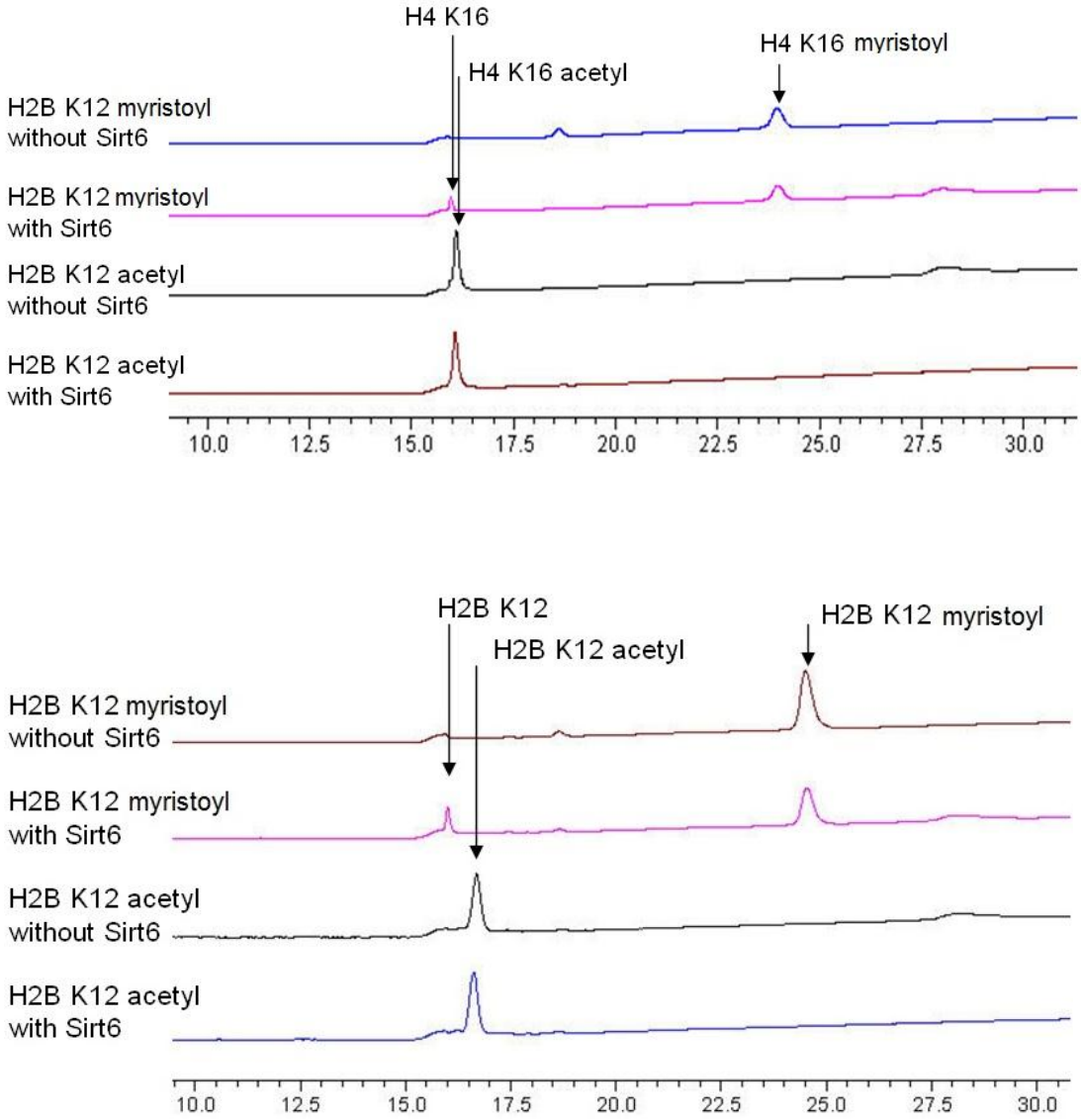

Fig. 2.7 HPLC traces for the hydrolysis of H2BK12 and H4K16 acetyl and myristoyl peptides by Sirt6 (1-314). The formation of demyristoylated peptides was confirmed using mass spectroscopy (data not shown here).

Once I fully confirmed the demyristoylation activity of the truncated Sirt6 (1-314), I also expressed the full length Sirt6 in *E. coli* strain of BL21DE3 ArcticExpress (AE) cells. My aim was to use different chain length H3K9 acyl peptides to test the same activity with the full length version of the protein and to determine the exact kinetic parameters for the same.

I re-established that the full length Sirt6 can hydrolyze long chain fattyacyl groups from WWH3K9 peptides much better than WWH3K9acetyl peptide as shown in Fig. 2.8A. Fig. 2.8B demonstrates that the full length Sirt6 can accommodate other peptide sequences also such as WWH2BK12myr. The activity found (Fig. 2.8A) was further confirmed by kinetic measurements (Table 2.2). The k_{cat}/K_m for demyristoylation (1400 $s^{-1}M^{-1}$) is approximately 300 times better than that for deacetylation (4.8 $s^{-1}M^{-1}$). The increased catalytic efficiency comes mainly from the decrease in K_m. The better binding affinity for longer chain fattyacyl groups is due to the presence of long hydrophobic pocket in the substrate binding pocket, which is absent in other sirtuins. For the acetyl peptide, the K_m value is 810 µM, but for demyristoylation, it is 3.4 µM.

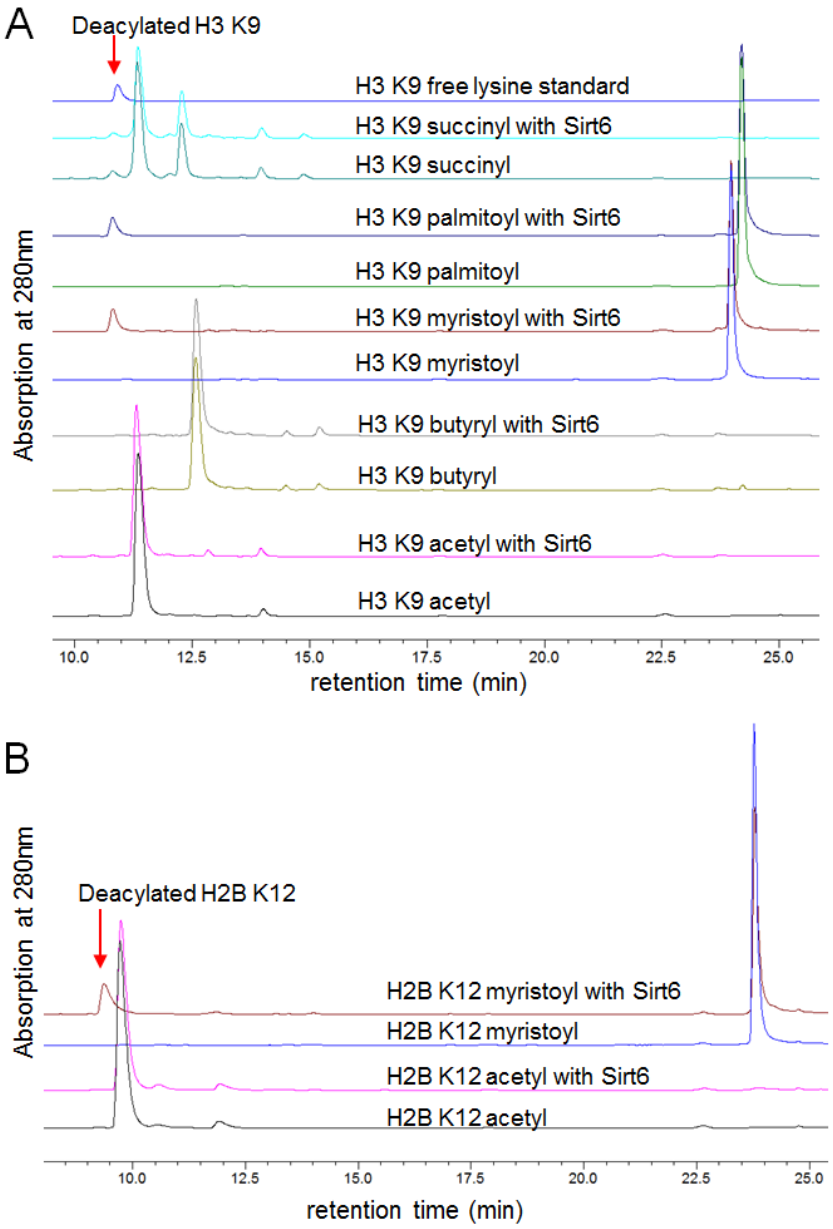

Fig. 2.8 Sirt6 prefers to hydrolyze long chain fattyacyl lysine *in vitro*. Panel A shows HPLC traces of Sirt6 catalyzed hydrolysis of different acyl peptides based on the H3K9 sequence. Panel B shows H2BK12 myristoyl peptide can be hydrolyzed by Sirt6 while the corresponding acetyl peptide cannot.

H3K9 Acyl peptide	k_{cat} (s^{-1})	K_m(μM)	k_{cat}/K_m($s^{-1}M^{-1}$)
Acetyl (C2)	0.0039±0.0006	810±160	4.8
Butyryl (C4)	0.0021±0.0004	200±120	10
Octanoyl (C8)	0.0046±0.0005	40±10	1.2×10^2
Myristoyl (C14)	0.0049±0.0004	3.4±0.9	1.4×10^3
Palmitoyl (C16)	0.0027±0.0002	0.9±0.4	3.0×10^3

Table 2.2 Catalytic efficiencies of Sirt6 on different acyl peptides.

In order to understand the preference of Sirt6 for medium and long chain fattyacyl groups, the truncated form of Sirt6, Sirt6 (1-294), was crystallized in collaboration with Yi Wang[*]. The Sirt6 (1-294) was complexed with H3K9myr peptide and ADP-ribose. The structure was determined at 2.2 Å resolution (Fig. 2.9) and it was found to be similar to the earlier published apo Sirt6 structure (34). However, residues 2-10 and 166-174 of Sirt6 are visible in the H3K9 myristoyl bound crystal structure, while the corresponding regions are missing in the published apo Sirt6 structure.

[*] Quan Hao, Yi Wang ,Department of Physiology, University of Hong Kong, Hong Kong, China

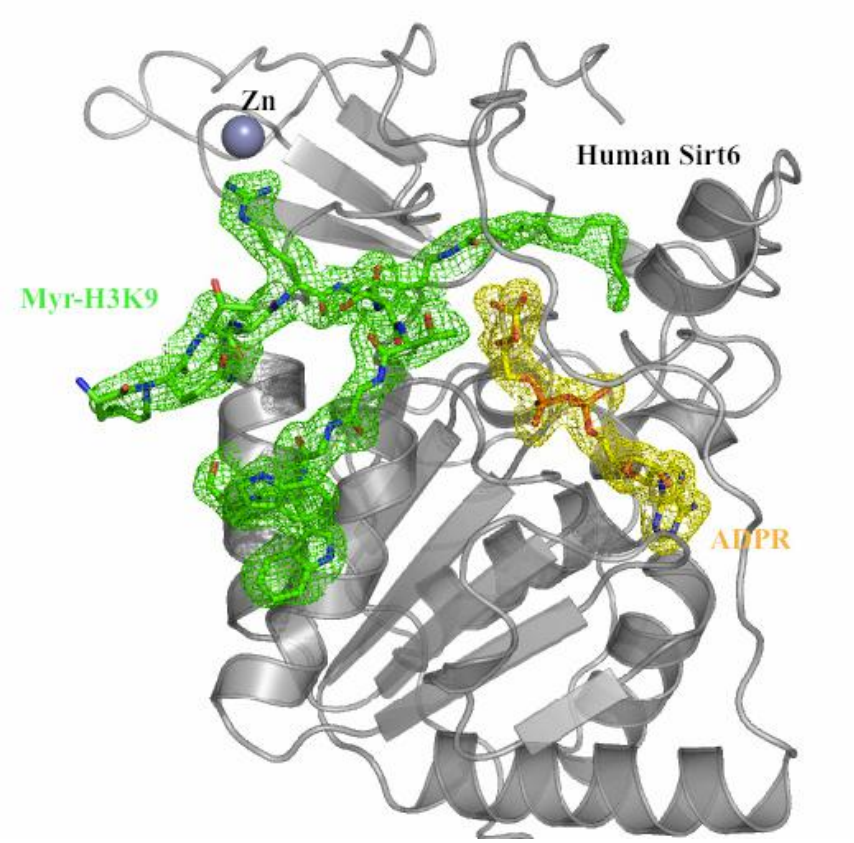

Fig. 2.9A Crystal structure of the full length Sirt6 complexed with H3K9myristoyl peptide (green) and ADP-ribose (yellow) at 2.2 Å resolution.

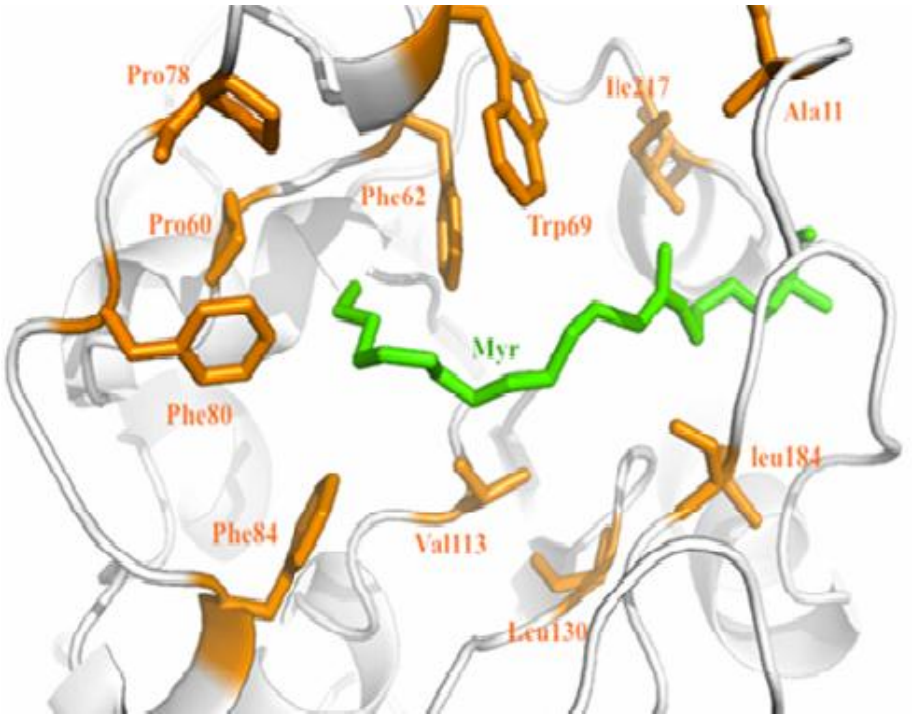

Fig. 2.9B Acyl pocket of the full length Sirt6 complexed with H3K9myristoyl peptide and ADP-ribose at 2.2 Å resolution. The residues highlighted in orange form hydrophobic pocket which can accommodate the myristoyl side chain shown in green.

There are two features in the crystal structure that explain the enzymology data. Firstly, the peptide interacts with Sirt6 through hydrogen bonding interactions similar to those observed in other sirtuins including Sirt5. Most of the hydrogen bonds come from the main chain C=O and N-H of the H3K9 myristoyl peptide, with the only side chain hydrogen bonding interactions coming from Trp11. Therefore, it appears that the selectivity for peptide sequences is not high. Secondly, the hydrophobic pocket, which accommodates the myristoyl group, is comprised of Ala11, Pro60, Phe62, Trp69, Pro78, Phe80, Phe84, Val113, Leu130, Leu184, and Ile217 hydrophobic residues. These residues form different flexible loops which are absent in other sirtuins.

The presence of fattyacyl CoAs in cells as metabolites and the fact that Sirt6 could efficiently remove long chain fattyacyl groups from lysine residues suggest that the lysine fattyacylation might be a more prevalent PTM than originally thought. Lysine myristoylation, although not widely known, was reported to occur in a few proteins such as interleukin α and TNFα (31, 32). Sirt6, known as a nuclear protein, was thought to remove modifications on histones (19, 20, 22). Also, there were reports that lysine propionylation and butyrylation occurred on the core histone H4 proteins (35). Proteomics study by Hang *et al.* suggested S-acylation might be present on some variants of H3 histones (36). With the backing of these findings, it was compelling to hypothesize that firstly, fattyacylation occurs on histone lysine residues and is an unrecognized epigenetic modification, and secondly, Sirt6 hydrolyzes the fattyacylation on histone lysines. Therefore, to seek the substrate for Sirt6, we focused on histones as a possible candidate. However, because lysine fattyacylation was not a very well recognized modification (9, 32), there were no antibodies present to probe this modification at the protein level.

At about the same time, Zhu *et al.* were studying PfSir2a (Sirt6 homolog in malaria parasite *Plasmodium falciparum*) and had detected a robust defattyacylation activity for H3K9 fattyacyl peptides (37). PfSir2a was more stable and sensitive in the radiolabeling assay than Sirt6 (1-314). This fact enabled us to use it for detecting whether or not lysine modification was present in histones. We started with the commercial calf thymus histone because it could be obtained easily in a reasonable quantity. Our goal was to digest the commercial calf thymus histone into peptides, and then test these digested peptides for fattyacylation mark using ^{32}P-NAD based biochemical radiolabeling assay.

The reason for the choice of ^{32}P-NAD biochemical radiolabeling assay was due to low levels of these modifications it could detect. The detection limits of this assay from the reaction of wwH3K9myristoyl peptide with pfSir2a and Sirt6 enzymes were found to be 0.03 μM peptide per 1 μM pfsir2a and 0.1 μM peptide per 1 μM Sirt6, respectively. The desired peptides would then be subjected to LC-MS/MS in order to confirm the modification. However, due to the hydrophobicity of the modification, we needed to modify and standardize the known techniques. The commercial calf thymus histone was trypsin digested and the digested mixture was desalted using sep pak C18 column (Waters Inc.). Using 50% and 90% acetonitrile-water, digested peptides were eluted as shown in Fig. 2.10a. The idea was to use a higher acetonitrile percentage (90% against the usual 50%) to elute more hydrophobic peptides. Elutions were also done using a blank cartridge as control.

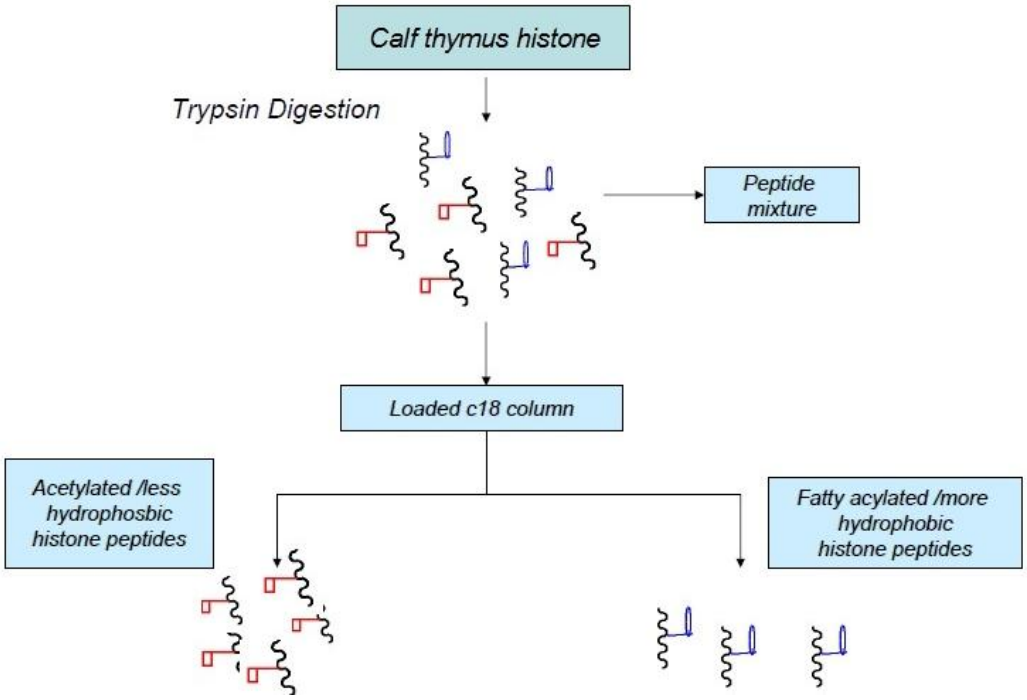

Fig. 2.10a Sample preparation for the detection of fattyacyl ADP-ribose from commercial calf thymus histones using trypsin digestion**.**

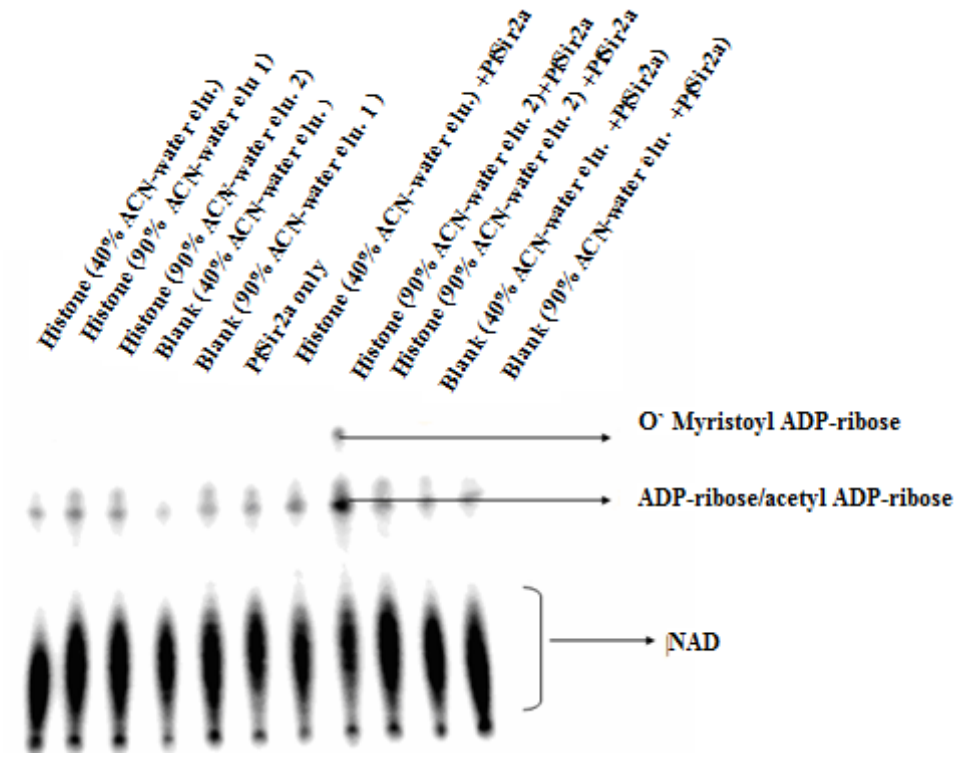

Fig. 2.10b ^{32}P-NAD radiolabeling assay with digested calf thymus histones shows the formation of fattyacyl ADP-ribose, when the 90% acetonitrile-water eluent is incubated with Sirt6 (1-314) and ^{32}P-NAD.

The peptides were lyophilized in glass vials (because hydrophobic peptides would stick to the plastic eppindorf tube). Dimethylsulfoxide was used for dissolving lyophilized peptides. ^{32}P-NAD radiolabeling biochemical assay was done with the recombinant pfSir2a as the defattyacylating enzyme. The idea was to see if we could observe the highly nonpolar 2´-O-fattyacyl ADP-ribose spot, since it would signify that fattyacylation is present on the calf thymus histones. It did show a highly non-polar fattyacyl ADP-ribose spot, which indicated that the commercial calf thymus histones might have the lysine fattyacylation (Fig. 2.10b). To confirm this, the digested peptides were subjected to LC-MS/MS using a gradient different from the one normally used. The gradient used went up to 90% acetonitrile-water. However, no fattyacylation could be detected. This

was mainly due to the inconsistency in fragmentation pattern for even the standard H3K9 myristoylated peptide and also the low abundance of the fattyacylated peptides.

Later on, my colleague Hong Jiang proposed that Sirt6 may regulate TNFα secretion via defattyacylation based on two reports (38, 39). These reports indicated that Sirt6 can regulate the synthesis of secreted TNFα. However, the mechanism was unclear. TNFα is a type II membrane protein with a single transmembrane domain connecting the intracellular N terminus with extracellular C terminus (40). It was already known that TNFα protein was myristoylated at Lys19 and Lys20 positions. Therefore, we hypothesized that Sirt6 may regulate TNFα secretion via defattyacylation. In order to test the hypothesis at the biochemical level, I synthesized a TNFα peptide with myristoyl modification at Lys19 and Lys20 positions and performed the kinetic study using the HPLC-based activity assay as described in Section 2.3. The catalytic efficiency (i.e. kcat/Km) was approximately 250 times higher than that for the H3K9 acetyl peptide and was similar to that for Sirt1 deacetylation (Table 2.3).

Peptide	k_{cat} (s^{-1})	K_m(μM)	k_{cat}/K_m($s^{-1}M^{-1}$)
TNFK20myristoyl	0.005±0.0004	4.5±1.1	1.1×10^3
TNFK19myristoyl	0.0020±0.0002	2.4±0.6	8.3×10^2

Table 2.3 Catalytic efficiencies of Sirt6 on TNFα peptides.

The rest of the experiments to test the hypothesis were performed by Hong Jiang and are described as follows. The hypothesis was tested on the cellular level by comparing the fattyacylation level of TNFα in Sirt6 WT MEF and Sirt6 KO MEF cells.

For this purpose, we used fattyacyl analogues to covalently label TNFα using a known scheme (41). The cells transfected with epitope tagged TNFα were cultured in the presence of fattyacyl analogues with an alkyne tag. The TNFα was then immuno-precipitated and conjugated to rhodamine azide using the click chemistry. The labeled or the fattyacylated proteins were visualized by fluorescence. To rule out the possibility of visualizing cysteine fattyacylation, the immuno-precipitated proteins were treated with hydroxyl amine in order to hydrolyze the cysteine fattyacylation prior to the visualization. Using fluorescence detection, it was found that WT TNFα obtained from the Sirt6 KO cells showed more labeling than that obtained from the Sirt6 WT MEF cells. It was also found that when mutating Lys19 and Lys20 of TNFα (sites of lysine myristoylation) to arginine, the labeling intensities dropped to the background level for the Sirt6 KO cells. This particular data confirmed the presence of lysine fattyacyl modifications at Lys19 and Lys20 residues of TNFα. Further, it was demonstrated in an *in vitro* assay that Sirt6 defattyacylation of TNFα (obtained from the Sirt6 KO MEF cells) was dependent on NAD^+. This data corroborated our finding from kinetic data on the TNFα peptides (Table 2.3) that Sirt6 defattyacylated TNFα through its NAD^+-dependent deacylation activity. Finally, to test the hypothesis that Sirt6 controlled TNFα secretion, FLAG-tagged TNFα was expressed in the Sirt6 KO and WT cells. The secretion efficiency was calculated by measuring the TNFα present in the cells and that present in media using ELISA based assay. The secretion efficiency was found to be less in Sirt6 KO MEF cells than the Sirt6 WT MEF cells. It was also found that the secretion of TNFα mutant did not show any difference in the WT and Sirt6 KO MEF cells. This established that the secretion is indeed controlled by the fattyacylation level of TNFα, which is in turn controlled by

defattyacylation activity of Sirt6. Since all the above studies were in the MEF cells with over expressed TNFα, the hypothesis was further extended on the endogenous TNFα obtained from the human acute monocytic leukemia (THP-1) cells and the mouse macrophages. Two Sirt6 KD cell lines were created using two short hairpin (sh) RNA and a control was generated using a control shRNA. Using the same labeling method as described above, it was observed that TNFα fattyacylation was higher in Sirt6 KD THP-1 cells than the control KD THP-1 cells. Using the ELISA assay, the amount of TNFα secreted in the media and the amount that remained in the cell were measured. Using the two values, the secretion efficiency was calculated. Secretion efficiency of TNFα was found to be greater in the Sirt6 KD THP-1 cell line in comparison to the control KD THP-1 cell line. Finally, to show that this finding is relevant at the cellular level, it was further demonstrated that Sirt6, which was thought to be a nuclear protein earlier, is also present in the endoplasmic reticulum, a central organelle for protein secretion.

2.5 Discussion

The biochemical and structural studies demonstrate that human Sirt6, which was known to have a weak deacetylase activity, can hydrolyze the longer chain fattyacyl groups much more efficiently than the shorter acetyl group. The kinetic parameters indicate that the defattyacylase activity of Sirt6 is comparable to the robust deacetylation activity of other sirtuins, Sirt1-3. The higher catalytic efficiency results from the lower K_m value. The mechanism for defattyacylation activity of Sirt6 is similar to the mechanism for deacetylation activity of other sirtuins. This is demonstrated by the biochemical radiolabeling assay and further confirmed by subjecting the isolated O-

fattyacyl-ADP-ribose intermediate to MALDI-TOF spectroscopy. However, the presence of longer catalytic pocket comprising of hydrophobic residues accommodates the fattyacyl modification, resulting in better binding affinity and robust defattyacylation activity. This long hydrophobic pocket is absent in other sirtuins, and therefore myristoyl or other fattyacyl groups are too long to fit in the catalytic pocket of most sirtuins.

Based on our work on histones and the recent report (36), it is possible that histones might be fattyacylated too. A further investigation with better detection techniques and LC-MS/MS methods might be helpful in exploring this idea. It is possible that the two activities, defattyacylation and deacetylation might work together depending on the conditions. We further demonstrate physiological relevance of this novel defattyacylase activity of Sirt6 in defattyacylating TNFα at Lys19/Lys20 position. This in turn regulates the secretion of TNFα. Since TNFα is central to many signaling pathways and is an important mediator of inflammation response, further investigations might shed light on role of Sirt6 in inflammation.

REFERENCES

1. Imai, S.-I., Armstrong, C. M., Kaeberlein, M., and Guarente, L., Transcriptional Silencing and Longevity Protein Sir2 is an NAD-Dependent Histone Deacetylase. *Nature* 403, 795-800 (2000).
2. Sauve, A. A., Wolberger, C., Schramm, V. L., and Boeke, J. D., The Biochemistry of Sirtuins. *Annu. Rev. Biochem.* 75, 435-465 (2006).
3. Michan, S. and Sinclair, D., Sirtuins in Mammals: Insights into their Biological Function. *Biochem. J.* 404, 1-13 (2007).
4. Kaeberlein, M., McVey, M., and Guarente, L., The SIR2/3/4 Complex and SIR2 Alone Promote Longevity in Saccharomyces Cerevisiae by Two Different Mechanisms. *Genes Dev.* 13, 2570-2580 (1999).
5. van der Horst, A., Tertoolen, L. G. J., de Vries-Smits, L. M. M., Frye, R. A., Medema, R. H., and Burgering, B. M. T., FOXO4 is Acetylated upon Peroxide Stress and Deacetylated by the Longevity Protein hSir2 SIRT1. *J. Biol. Chem.* 279, 28873-28879 (2004).
6. Tissenbaum, H. A. and Guarente, L., Increased Dosage of a Sir-2 Gene Extends Lifespan in Caenorhabditis Elegans. *Nature* 410, 227-230 (2001).
7. Howitz, K. T., *et al*., Small Molecule Activators of Sirtuins Extends *Saccharomyces Cervisiae* Life Span. *Nature* 425, 191-196 (2003).
8. Picard, F., Kurtev, M., Chung, N., Topark-Ngarm, A., Senawong, T., Machado de Oliveira, R. *et al*., SirT1 Promotes Fat Mobilization in White Adipocytes by Repressing PPAR-gamma. *Nature* 429, 771-776 (2004).

9. Mostoslavsky, R., Chua, K. F., Lombard, D. B., Pang, W. W., Fischer, M. R., Gellon, L. *et al*., Genomic Instability and Aging-Like Phenotype in the Absence of Mammalian SIRT6. *Cell* 124, 315-329 (2006).
10. Ford, E., Voit, R., Liszt, G., Magin, C., Grummt, I., and Guarente, L., Mammalian Sir2 Homolog SIRT7 is an Activator of RNA Polymerase I Transcription. *Genes Dev.* 20, 1075-1080 (2006).
11. Motta, M. C., Divecha, N., Lemieux, M., Kamel, C., Chen, D., Gu, W. *et al*., Mammalian SIRT1 Represses Forkhead Transcription Factors. *Cell* 116, 551-563 (2004).
12. Bouras, T., Fu, M., Sauve, A. A., Wang, F., Quong, A. A., Perkins, N. D. *et al.*, SIRT1 Deacetylation and Repression of p300 Involves Lysine Residues 1020/1024 within the Cell Cycle Regulatory Domain 1. *J. Biol. Chem.* 280, 10264-10276 (2005).
13. Qiao, L. and Shao, J., SIRT1 Regulates Adiponectin Gene Expression through Foxo1-C/Enhancer-Binding-Protein Transcriptional Complex. *J. Biol. Chem.* 281, 39915-39924 (2006).
14. Rodgers, J. T., Lerin, C., Haas, W., Gygi, S. P., Spiegelman, B. M., and Puigserver, P., Nutrient Control of Glucose Homeostasis through a Complex of PGC-1 Alpha and SIRT1. *Nature* 434, 113-118, March 3 (2005).
15. Haigis, M. C., Mostoslavsky, R., Haigis, K. M., Fahie, K., Christodoulou, D. C., Murphy, A. J. *et al*., SIRT4 Inhibits Glutamate Dehydrogenase and Opposes the Effects of Calorie Restriction in Pancreatic β-Cells. *Cell* 126, 941-954 (2006).

16. Nakagawa, T., Lomb, D. J., Haigis, M. C., and Guarente, L., SIRT5 Deacetylates Carbamoyl Phosphate Synthetase 1 and Regulates the Urea Cycle. *Cell* 137, 560-570 (2009).

17. Kim, H.-S., Xiao, C., Wang, R.-H., Lahusen, T., Xu, X., Vassilopoulos, A. *et al*., Hepatic-Specific Disruption of SIRT6 in Mice Results in Fatty Liver Formation Due to Enhanced Glycolysis and Triglyceride Synthesis. *Cell Metabolism* 12, 224-236 (2010).

18. Zhong, L., D'Urso, A., Toiber, D., Sebastian, C., Henry, R. E., Vadysirisack, D. D. *et al.*, The Histone Deacetylase Sirt6 Regulates Glucose Homeostasis via Hif1[alpha]. *Cell* 140, 280-293 (2010).

19. Michishita, E., McCord, R. A., Boxer, L. D., Barber, M. F., Hong, T., Gozani, O. *et al*., Cell Cycle-Dependent Deacetylation of Telomeric Histone H3 Lysine K56 by Human SIRT6. *Cell Cycle* 8, 2664-2666 (2009).

20. Michishita, E., McCord, R. A., Berber, E., Kioi, M., Padilla-Nash, H., Damian, M. *et al*., SIRT6 is a Histone H3 Lysine 9 Deacetylase that Modulates Telomeric Chromatin. *Nature* 452, 492-496 (2008).

21. Liszt, G., Ford, E., Kurtev, M., and Guarente, L., Mouse Sir2 Homolog SIRT6 is a Nuclear ADP-Ribosyltransferase. *J. Biol. Chem.* 280, 21313-21320 (2005).

22. Michishita, E., Park, J. Y., Burneskis, J. M., Barrett, J. C., and Horikawa, I., Evolutionarily Conserved and Non-Conserved Cellular Localizations and Functions of Human SIRT Proteins. *Mol. Biol. Cell* 16, 4623-4635 (2005).

23. Du, J., Zhou, Y., Su, X., Yu, J., Khan, S., Jiang, H. *et al.*, SirT5 is an NAD-Dependent Protein Lysine Demalonylase and Desuccinylase. *Science* 334, 806-809 (2011).

24. Zhang, Z., Tan, M., Xie, Z., Dai, L., Chen, Y., and Zhao, Y., Identification of Lysine Succinylation as a New Post-Translational Modification. *Nat. Chem. Biol.*, 58-63, Jan. 7 (2011).

25. Xiao, C., Kim, H.-S., Lahusen, T., Wang, R.-H., Xu, X., Gavrilova, O. *et al.*, SIRT6 Deficiency Results in Severe Hypoglycemia by Enhancing both Basal and Insulin-Stimulated Glucose Uptake in Mice. *J. Biol. Chem.* 285, 36776-36784 (2010).

26. Kanfi, Y., Naiman, S., Amir, G., Peshti, V., Zinman, G., Nahum, L. *et al.*, The Sirtuin SIRT6 Regulates Lifespan in Male Mice. *Nature* 483, 218-221 (2012).

27. Yang, B., Zwaans, B. M. M., Eckenslorff, H., and Lombard, D. B., Sirtuin Sirt6 Deacetylates H3K56Ac in vivo to Promote Genomic Stability. *Cell Cycle* 8, 2662-2663 (2009).

28. Kawahara, T. L. A., Michishita, E., Adler, A. S., Damian, M., Berber, E., Lin, M. *et al.*, SIRT6 Links Histone H3 Lysine 9 Deacetylation to NF-[kappa]B-Dependent Gene Expression and Organismal Life Span. *Cell* 136, 62-74 (2009).

29. Mostoslavasky, R., Lombard, D. B. *et al.*, The Histone Deacetylase Sirt6 is a Tumor Suppressor that Controls Cancer Metabolism. *Cell* 151, 6, 1185-1199, Dec. 7 (2012).

30. Schwer, B., Schumacher, B., Lombard, D. B., Xio, C., Kurtev, M. V., Gao, J., Schneider, J. I., Chai, H., Bronsen, R. T., Tsi, L. H., Deng, C. X., Alt, F. W.,

Neural Sirtuin6(Sirt6)ablation Attenuates Somatic Growth and Causes Obesity. *Proc. Natl. Acad. Sc. U. S. A.* 107(50), 21790-4, Dec. 14 (2010).

31. Stevenson, F. T., Bursten, S. L., Locksley, R. M., and Lovett, D. H., Myristoyl Acylation of the Tumor Necrosis Factor Alpha Precursor on Specific Lysine Residues. *J. Exp. Med.* 176, 1053-1062 (1992).
32. Stevenson, F. T., Bursten, S. L., Fanton, C., Locksley, R. M., and Lovett, D. H. The 31-kDa Precursor of Interleukin 1 Alpha is Myristoylated on Specific Lysines within the 16-kDa N-Terminal Propiece. *Proc. Natl. Acad. Sci. U. S. A.* 90, 7245-7249 (1993).
33. Kates, S. A., Daniels, S. B., Albericio, F., Automated Allyl Cleavage for Continuous – Flow Synthesis of Cyclic and Branched peptides, *Analytical Biochemistry* 212, 303-310 (1993).
34. Pan, P. W., Feldman, J. L., Devries, M. K., Dong, A., Edwards, A. M., and Denu, J. M., Structure and Biochemical Functions of SIRT6. *J. Biol. Chem.* 286, 14575-14587 (2011).
35. Chen, Y., Sprong, R., Tana, Y., Bali, H., Sangras, B., Kim, S. C., Flack, J. R., Peng, J. G. W., and Zhaoy, Y., Lysine Propionylation and Butyrylation are Lower Post-Translational Modifications in Histones. *Mol. Cell Proteomics* 6(5), 812-9, May (2007).
36. Wilson, J. P., Raghavan, A. S., Yang, Y.-Y., Charron, G., and Hang, H. C., Proteomic Analysis of Fatty-Acylated Proteins in Mammalian Cells with Chemical Reporters Reveals S-Acylation of Histone H3 Variants. *Mol. Cell. Proteomics* 10, (2011).

37. Zhu, A. Y., Zhou, Y., Khan, S., Deitsch, K. W., Hao, Q., and Lin, H., Plasmodium Falciparum Sir2A Preferentially Hydrolyzes Medium and Long Chain Fattyacyl Lysine. *ACS Chem. Biol.* 7, 155-159 (2011).

38. Van Gool, F., Galli, M., Gueydan, C., Kruys, V., Prevot, P.-P., Bedalov, A. *et al*., Intracellular NAD Levels Regulate Tumor Necrosis Factor Protein Synthesis in a Sirtuin-Dependent Manner. *Nat. Med.* 15, 206-210 (2009).

39. Bruzzone, S., Fruscione, F., Morando, S., Ferrando, T., Poggi, A., Garuti, A. *et al*., Catastrophic NAD Depletion in Activated T Lymphocytes through Nampt Inhibition Reduces Demyelination and Disability in EAE. *PLoS ONE* 4, e7897 (2009).

40. Locksley, R. M., Killen, N., and Lenardo, N. J., The TNF and TNF Receptor Super Families: Integrating Mammalian Biology. *Cell* 104(4), 487-501, Feb. 23 (2001).

41. Charron, G., Zhang, M. M., Yount, J. S., Wilson, J., Raghavan, A. S., Shamir, E. et al., Robust Fluorescent Detection of Protein Fatty-Acylation with Chemical Reporters. *J. Am. Chem. Soc*. 131, 4967-4975 (2009).

CHAPTER 3

Study of Defattyacylase Activity of Sirt6: Partial Results and Possible Extensions

3.1 Introduction

The sirtuin family of enzymes has been known as NAD-dependent deacetylases, though some of them have very weak or no detectable deacetylase activity. Sirt6 is important for DNA repair, transcription, metabolism, and life span expansion mainly because of its deacetylase activity. In Chapter 2, I showed that Sirt6 possesses a new activity by removing long chain fattyacyl group from protein lysine residues and has a role in promoting TNFα secretion (1). In this chapter, I mainly studied two extensions of the previous work related to the defattyacylase activity of Sirt6:

1. *To obtain Sirt6 mutants responsible for the defattyacylase activity* - In the crystal structure shown in the previous chapter (Fig. 2.9B), the acyl pocket for Sirt6 contains a number of hydrophobic residues. My aim was to mutate some of these residues, namely Leu9 (not shown in Fig. 2.9B), Phe82, Phe86, and Val115 to the more hydrophilic residue arginine and to check the effect of these mutations on the preference of Sirt6 for long chain acyl peptides. Finally, we wanted to test the effects of these mutants on TNFα secretion. The goal was to identify an inactive mutant.
2. The recent reports by Garabunova *et al.* (2, 3) showed that Sirt6 promoted DNA repair during oxidative stress by activating Poly ADP-ribose polymerase-1 (PARP-1). This function has been attributed to the ADP-ribosoyl transferase activity of Sirt6, which was earlier thought to be too weak to be relevant in the

physiological context (4, 5). It was reported that during oxidative stress, Sirt6 activates PARP-1 by mono-ADP-ribosylating it. PARP-1 would in turn ADP-ribosylate itself and other proteins, thereby promoting DNA DSB repair. I wanted to explore the efficiency of the self ADP-ribosylation activity of Sirt6 in comparison to the diphtheria toxin (DT) catalyzed ADP-ribosylation of elongation factor 2 (EF-2). I was also interested in knowing whether the mutants G60A and R65A mentioned above would affect the defattyacylase activity and whether it is possible that Sirt6 regulates PARP-1 by defattyacylation instead of mono-ADP-ribosylation.

3.2 Methods

Cloning and Transformation

The mutation in hSirt6 gene L9R was done using the stratagene quickchange method as described in the manual (6) except for the transformation part. The dsDNA template used was hSirt6 in pET28a (+) vector. The cycling parameters were taken from the Stratagene manual and the extension time used was 6 min. The mutated plasmid was digested using Dpn1 enzyme for 1 h at 37 ºC and 1 µL of the Dpn1 digested reaction mixture was transformed into Lucigen 10 G Solo chemically competent cells. The successful transformants were selected by plating the cells on kanamycin (50 mg/ml) Luria broth (LB) plates. The presence of the mutated gene was confirmed using Sanger/3730XL DNA sequencing. The primers used are described below and were purchased from Integrated DNA Technology (IDT).

SK009Sirt6L9R5’gaattacgcggcggggCGTtcgccgtacgcggacaag;

SK010Sirt6L9R3’ cttgtccgcgtacggcgaACGccccgccgcgtaattc.

The other two single mutations in Sirt6 gene, V115R and F82R, were prepared by the overlap extension PCR method using Accuprime pfx enzyme (Invitrogen). The mutated gene was cloned into pET28 a (+) vector between the BamH1 and Not1 restriction sites and ligated using quick ligase enzyme. The Sirt6 single mutant expression vectors were transformed into Lucigen 10 G solo chemically competent cells and selected by plating the cells on kanamycin (50 mg/ml) LB plates. The presence of the mutated gene was confirmed using Sanger/3730XL DNA sequencing. The primers used are listed below and were purchased from IDT.

V115RSK0175’; cttcctggtcagccagaacCGTgacgggctccatgtgcgc;

V115RSK0183’; gttctggctgaccaggaag;

F82RSK019 5’;cgaggtctggcccccaagCGTgacaccacctttgagagcg;

F82RSK0203’;Cttgggggccagacctcg;

SK001S56Y 5’ cacacgggtgccggcatcTACactgcctctggcatcccc;

SK002 3’ gatgccggcacccgtgtg;

SK005G60A 5’ ggcatcagcactgcctctGCC atccccgacttcaggggtc;

SK006 G60AG3’ agaggcagtgctgatgcc;

SK007 H133Y 5’ ggacaaactggcagagctcTAC gggaacatgtttgtggaagaa;

SK008 H133Y3’ gagctctgccagtttgtcc;

SKR65A0245'; ctctggcatccccgacttcGCCggtccccacggagtctgg;

SKR65A025 3'; gaagtcggggatgccagag;

Transformation in ArcticExpress Cells

The hSirt6 mutant expression vectors were transformed in the *E. coli* Rosetta ArcticExpress (DE3) cells at 42 °C for 90 s followed by recovery with 900 µL of 2 × YT media. The successful transformants were selected by plating the cells on kanamycin (50 mg mL^{-1}) and gentamycin (10 mg mL^{-1}) LB plates. Single colonies were selected and grown in 2 × YT media with kanamycin (50 mg mL^{-1}) and gentamycin (10 mg mL^{-1}) as antibiotics overnight at 37 °C. On the following day, the cells were sub-cultured (1:1000 dilution) into 2 L of 2 × YT media with kanamycin (50 mg mL^{-1}) and gentamycin (20 mg mL^{-1}). To induce the expression of desired protein, the cell culture was cooled to 12 ºC and isopropyl-d-1-thiogalactopyranoside (IPTG) was added to a final concentration of 0.2 mM when OD_{600} was 0.6 - 0.8. The culture was grown for another 40 h at 12 ºC.

Purification

Cells were harvested by centrifugation at 7,330 g for 10 min at 4 °C and then resuspended in lysis buffer (20 mM Tris-HCl, pH 7.2, 500 mM NaCl and 2% glycerol, 10 µL buffer saturated PMSF solution in ethanol per 50 ml lysis buffer). The suspension was lysed using an EmulsiFlex-C3 cell disruptor (AVESTIN Inc.) and then centrifuged at 29,300 g for 35 min at 4 ºC in order to remove the cell debris. The supernatant was loaded into the column pre-equilibrated with Ni-NTA resin (Qiagen) in lysis buffer. The target protein was eluted using 100 mM imidazole solution in 20 mM Tris-HCl pH 7.2, 500 mM NaCl and 2% glycerol. The desired fractions were pooled, concentrated, and buffer exchanged against the cation exchange buffer (80 mM NaCl, 20 mM Tris pH 7.2, 2% glycerol). The protein was then loaded onto a cation exchange column (Amersham

Biosciences) and was eluted with 1 M NaCl, 20 mM Tris-HCl, pH 7.2, 2% glycerol. Fractions were assayed for purity on SDS-PAGE gel and were concentrated and stored at -80 ºC.

Activity Assay

Activities of Sirt6 mutants S56Y, R65A, G60A, and H133Y were determined using HPLC to separate the reaction mixture detecting the modified and unmodified WWH3K9 peptide. The reaction mixture comprised of 20 mM of Tris pH 8.0, 1 mM DTT, 50 μM WWH3K9 modified peptide, 0.5 mM of NAD, and 2.8 μM of Sirt6 mutants and was incubated at 37 ºC for 1 h. The reaction was stopped with 1 equivalent of 0.5 N HCl in methanol and spun down for 10 min at 18,000 g (Beckman Coulter Microfuge) to separate the protein from the reaction mixture. The supernatant was then analyzed by HPLC using the unmodified WWH3K9 peptide as a standard for the decaylation product.

Kinetic Assay for Acetyl and Butyryl Peptides

The acetyl or butyryl peptides were dissolved in 25% DMSO water mixture. The concentrations of peptides were determined at 280 nm using extinction coefficient of the two tryptophan residues attached at the C terminus of the peptides (since the tryptophan residues added to the peptides absorb predominantly at this wavelength). The final DMSO concentration in the reaction mixture was maintained to be 2.5 %. Peptide concentrations were varied from 0 to 250 μM for WWH3K9 butyryl peptide and from 0 to 600 μM for the WWH3K9 acetyl peptide. The reactions containing 2 mM NAD, 1 mM DTT, 20 mM Tris, pH 8.0, 4 μM recombinant full length Sirt6, and acyl peptides at various

concentrations were incubated for 30 min at 37 °C. The reactions were stopped using 1 volume of 0.5 N HCl in methanol. The reaction mixtures were spun at 18,000 g for 10 min and were analyzed using a Kinetex XB-C18 column (100 Å, 100 mm × 4.60 mm, 2.6 μm, Phenomenex). The gradient of 20-40% B in 17 min at 0.5 mL/min was used. The product peak and the substrate peak were quantified using absorbance at 280 nm and converted to initial rates. Initial rates were then plotted against the acyl peptide concentration and fitted using the software KaleidaGraph.

Kinetic Assay for Long Chain Fattyacyl Peptides

The longer chain fattyacyl peptides were dissolved in pure DMSO. The concentrations of peptides were determined at 280 nm using extinction coefficient of the two tryptophan residues attached at the C terminus of the peptides (since the tryptophan residues added to the peptides absorb predominantly at this wavelength). The final DMSO concentration in the reaction mixtures was maintained to be 2.5%. The peptide concentrations were varied from 1 to 20 μM. The reactions containing 2 mM NAD, 1 mM DTT, 20 mM Tris pH 8.0, 0.2 μM recombinant full length Sirt6, and acyl peptides at different concentrations were incubated for 15 min at 37 °C. The reactions were stopped using 1 volume of 0.5 N HCl in methanol. The reaction mixtures were spun at 18,000 g for 10 min and were analyzed using a Kinetex XB-C18 column (100 Å, 75 mm × 4.60 mm, 2.6 μm, Phenomenex). The gradient of 0-55% B in 10 min at 0.5 ml//min was used. The product peak and the substrate peak were quantified using absorbance at 280 nm and converted to initial rates. Initial rates were then plotted against the acyl peptide concentration and fitted using the software KaleidaGraph.

3.3 Results

The hydrophobic residues of Sirt6 enveloping the myristoyl backbone were mutated to the hydrophilic residue arginine. Our aim was to mutate the residues Leu9, Phe82, Phe86, and Val115 to find out whether these four mutants would have decreased defattyacylase activity. However, I could only obtain three of the mutants, L9R, F82R and V115R. Cloning was done using stratgene quickchange method (6) for the L9R mutant because the mutation was very close to the 5´ restriction site. V115R and F82R were cloned using the PCR overlap extension method. The details of the two cloning methods are described in the previous section. Fig. 3.1a - 3.1c show the purification of various Sirt6 mutant proteins in AE cells. The expected molecular weight of the proteins is approximately 39.9 kDa.

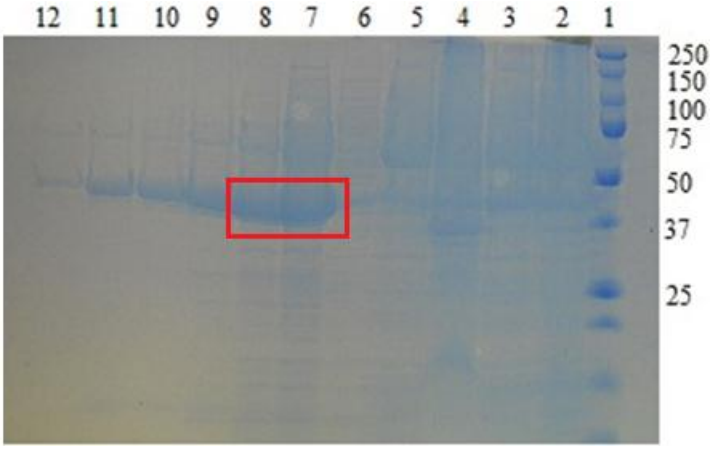

Fig. 3.1a The purification of Sirt6 L9R mutant protein using Ni-NTA affinity purification. The Coomassie blue stained gel shows elutions obtained from Ni-NTA purification using different concentrations of imidazole solutions to obtain the Sirt6 L9R His_6 –tagged protein. The protein was further subjected to cation exchange purification (not shown here). Lane key: Lane 1: Protein standard; 2: Cell lysate; 3: Supernatant; 4: Inclusion bodies; 5: Flow through; 6: 25 mM imidazole; 7: 100 mM imidazole –elution 1; 8: 100 mM imidazole –elution 2; 9: 150 mM imidazole elution- 1; 10: 150 mM imidazole –elution 2; 11: 200 mM imidazole –elution 1; 12: 200 mM imidazole elution- 2. The eluted protein is show in the red box.

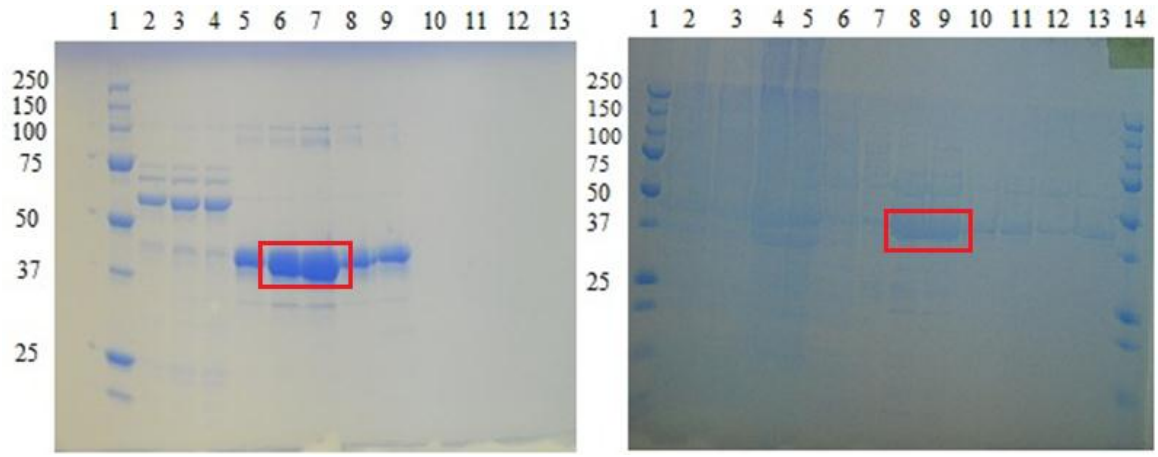

Fig. 3.1b The purification of Sirt6 F82R mutant protein using Ni-NTA affinity purification in the right panel. Left panel shows the fractions obtained from the cation exchange purification performed after the Ni-NTA purification. Right panel shows the Coomassie blue stained gel shows elutions obtained from Ni-NTA purification using different concentrations of imidazole solutions to obtain the Sirt6 F82R His_6 –tagged protein. The protein was further subjected to cation exchange purification shown in the left panel. Right Panel Lane key: Lane 1: Protein standard; 2: Cell lysate; 3: Supernatant; 4: Inclusion bodies; 5: Flow through; 6: 25 mM imidazole elution-1; 7: 25 mM imidazole elution-2 8: 100 mM imidazole elution- 1; 9: 100 mM imidazole elution-2; 10: 150 mM imidazole elution-1; 11: 150 mM imidazole –elution 2; 12: 200 mM imidazole elution-1; 13: 200 mM imidazole elution-2. Left Panel shows the fractions obtained from cation exchange resin purification, fractions 7 and 8 combined. The eluted protein is show in the red box.

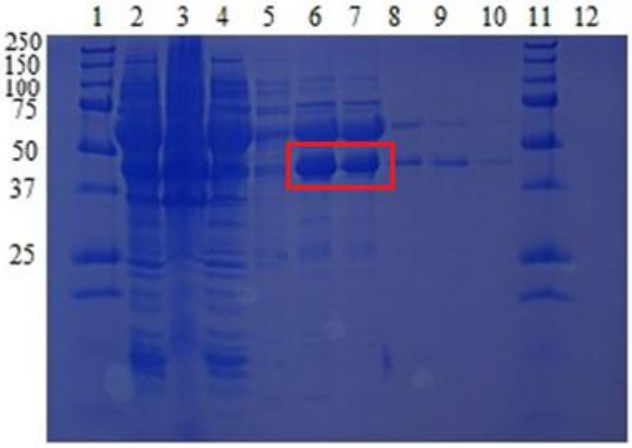

Fig. 3.1c The purification of Sirt6 V115R mutant protein using Ni-NTA affinity purification. The Coomassie blue stained gel shows elutions obtained from Ni-NTA purification using different concentrations of imidazole solutions to obtain the Sirt6 V115R His_6 –tagged protein. Lane key: Lane 1: Protein standard; 2: Cell lysate; 3:

Supernatant; 4: Flow through; 5: 25 mM imidazole; 6: 100 mM imidazole –elution 1; 7: 100 mM imidazole –elution 2; 8: 150 mM imidazole elution- 1; 9: 150 mM imidazole – elution 2; 10: 200 mM imidazole –elution 1; 11: Protein standard. The 100 mM elution fractions were collected and further subjected to cation exchange purification (not shown). The eluted protein is show in the red box.

Fig. 3.1d The purification of Sirt6 R65A mutant protein was performed using Ni-NTA affinity purification followed by the cation exchange purification. The Coomassie stained blue gel shows fractions obtained from the cation exchange purification. The fractions 6 and 8 were collected; the expected weight of the proteins is 39.9 kDa. The eluted protein is show in the red box.

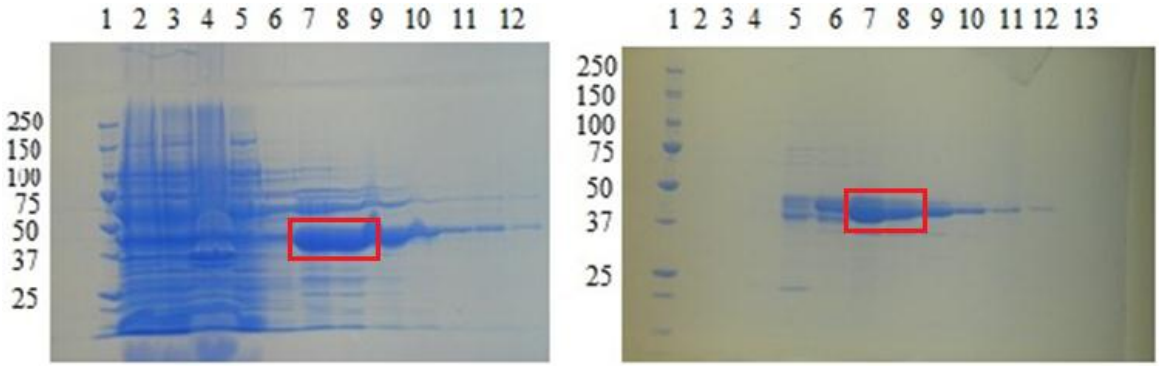

Fig. 3.1e The purification of Sirt6 H133Y mutant protein using Ni-NTA affinity purification (left) and cation exchange purification (right). The Coomassie blue stained gel on left shows elutions obtained from Ni-NTA purification using different concentrations of imidazole solutions to obtain the Sirt6 H133Y His_6 –tagged protein. Lane key: Lane 1: Protein standard; 2: Cell lysate; 3: Supernatant; 4: Inclusion bodies; 5: Flow through; 6: 25 mM imidazole elution-1; 7: 100 mM imidazole elution- 1; 8: 100 mM imidazole elution-2; 9: 150 mM imidazole elution-1; 10: 150 mM imidazole –elution

2; 11: 200 mM imidazole elution-1; 12: 200 mM imidazole elution-2. Right panel shows fractions obtained from the cation exchange purification. Fractions 7 and 8 were collected. The eluted protein is show in the red box.

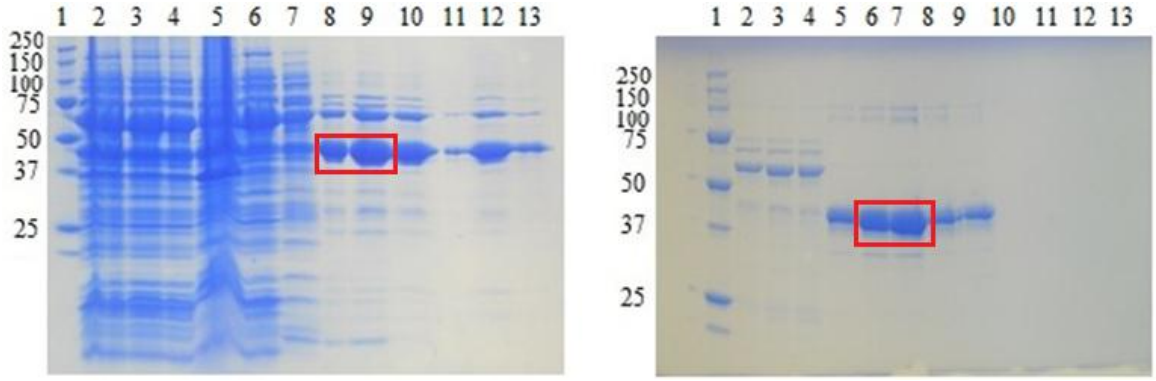

Fig. 3.1f The purification of Sirt6 G60A mutant protein using Ni-NTA affinity purification (left) and cation exchange purification (right). The Coomassie blue stained gel on left shows elutions obtained from Ni-NTA purification using different concentrations of imidazole solutions to obtain the Sirt6 G60A His_6 –tagged protein. Lane key: Lane 1: Protein standard; 2: Cell lysate; 3: Supernatant; 4: Inclusion bodies; 5: Flow through; 6: 25 mM imidazole elution-1; 7: 25 mM imidazole elution-1; 8: 100 mM imidazole elution- 1; 9: 100 mM imidazole elution-2; 10: 150 mM imidazole elution-1; 11: blank (some leaking from adjoining lane); 12: 150 mM imidazole elution-1; 13: 200 mM imidazole elution-1. Right panel shows fractions obtained from the cation exchange purification. Fractions 7 and 8 were collected. The eluted protein is show in the red box.

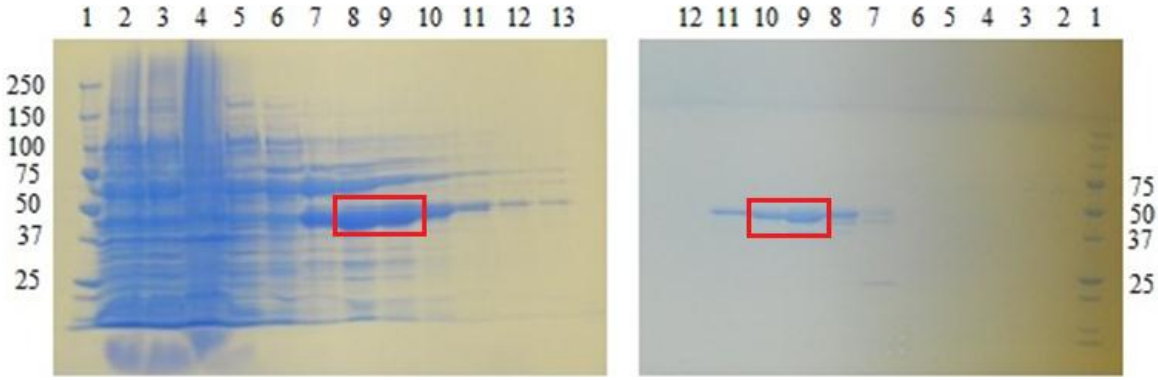

Fig. 3.1g The purification of Sirt6 S56Y mutant protein using Ni-NTA affinity purification (left) and followed by the cation exchange purification (right). The Coomassie blue stained gel shows elutions obtained from Ni-NTA purification using different concentrations of imidazole solutions to obtain the Sirt6 S56Y His_6 –tagged protein. The protein was further subjected to cation exchange purification (not shown here). Lane key: Lane 1: Protein standard; 2: Cell lysate; 3: Supernatant; 4: Inclusion bodies; 5: Flow through; 6: 25mM imidazole elution-1; 7: 25mM imidazole elution-2; 8:

100 mM imidazole –elution 1; 9: 100 mM imidazole –elution 2; 10: 150 mM imidazole elution- 1; 11: 150 mM imidazole –elution 2; 12: 200 mM imidazole –elution 1; 13: 200 mM imidazole elution- 2. Right panel shows fractions obtained from the cation exchange purification. Fractions 7 and 8 were collected. The eluted protein is show in the red box.

Fig. 3.1 The various Sirt6 mutant proteins purified in AE cells. The expected weight of the proteins is 39.9 kDa.

HPLC based activity assays as described in the previous chapter need to be performed to assess the decaetylation and the defattyacylation activity of these mutants (namely L9R, F82R and V115R). Kinetic measurements for both deacetylation and defattyacylation will be helpful in identifying the inactive mutant for the novel defattyacylase activity.

Another question we wanted to address was whether the mutants – G60A, R65A, H133Y, and S56Y, which have been well described in literature (2, 3), would have any effect on the novel defattyacylase activity. Towards this end, we cloned the above mentioned mutants using the PCR overlap extension method as described in Section 3.2. The proteins were expressed in the BL21R2 AE strain of the *E. coli* cells. Fig. 3.1d - 3.1g shows the purification for the mutant proteins.

We then assessed the demyristoylation activity of these mutants using an HPLC based assay for obtaining the kinetic parameters. No demyristoylation was observed with the Ser6Tyr mutant. The G60A and H133Y mutants showed demyristoylation activity. A preliminary analysis of the kinetic parameters of the demyristoylation activity for the two is as follows: for G60A, the k_{cat}/K_m was 4.08×10^3 $M^{-1}s^{-1}$ and for H133Y, the value was 4.75×10^2 $M^{-1}s^{-1}$. Considering these rough estimates, the demyristoylation activity of the two mutant proteins appears to be similar to Sirt6 WT demyristoylation activity. On the

other hand, the k_{cat}/K_m for the deacetylation activity of G60A, which is known to stop the mono-ADP-ribosyltransferase activity, was found to be 4.71 $M^{-1}s^{-1}$. This is similar to the k_{cat}/K_m of deacetylation activity for Sirt6 WT. Further investigation is required to determine the kinetic parameter for the mutant R65A, which has been proposed in literature (2) to be responsible for abrogating the deacetylase activity (2, 3), especially in relation to the novel defattyacylase activity. However, more extensive study is needed to prove the relevance of these amino acids with respect to defattyacylase activity.

It has also been reported in literature that Sirt6 ADP-ribosylates PARP-1 in response to the oxidative stress, thereby promoting the repair of DSBs (2, 3). Therefore, we were also interested in comparing how strong self ADP-ribosylation activity of Sirt6 compared to the robust ADP-ribosylation of EF-2 by DT. Briefly, it was done by incubating the Sirt6 with ^{32}P-NAD. The autoradiograph in Fig. 3.2 shows strong labeling for the DT catalyzed ADP-ribosylation of EF-2 compared to the self mono-ADP-ribosylation of Sirt6. The comparison was done based on equal moles of substrates taken, i.e., Sirt6 and EF-2.

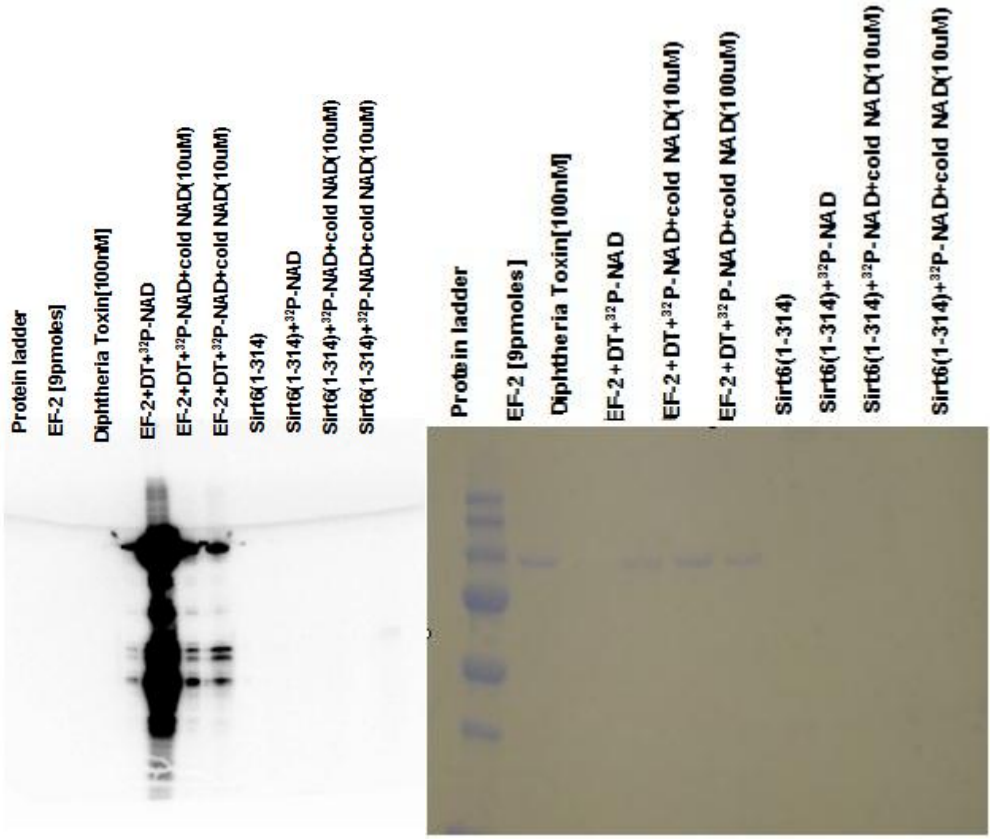

Fig. 3.2 Comparison of DT catalyzed ADP-ribosylation of EF-2 with self ADP-ribosylation of Sirt6; left panel shows the autoradiograph of the ^{32}P-NAD assay for the assessing ADP-ribosylation activity of Sirt6; right panel shows the commassie blue gel. Sirt6 protein is not visible on the gel due to low concentration (9 pmolar)

3.4 Discussion

Our work in the previous chapter showed that Sirt6 is a more efficient defattyacylase than a deacetylase. Next, we wanted to explore the importance of some of the hydrophobic residues present in the acyl pocket of Sirt6. We also wanted to identify an inactive mutation which would abrogate the defattyacylase activity. We successfully cloned, expressed, and purified the mutant proteins. However, more experiments (specifically activity assay and kinetic assay) need to be done to confirm the inactive mutant and to study its effect on the TNFα secretion.

Gorbunova *et al.* recently suggested that PARP-1 is ADP-ribosylated by Sirt6. The study pointed out some mutations such as G60A and R65A specifically abrogate the ADP-ribosyl transferase and the NAD-dependent deacetylase activities, respectively. We wanted to assess the efficiency of the ADP-ribosyltransferase activity of Sirt6 in comparison to the robust ADP-ribosyltransferase activity of other proteins (i.e. diptheria toxin catalyzed ADP-ribosylation on elongation factor-2). We also wanted to study how the mutants would affect the defattyacylase assay for Sirt6. We were partially able to determine the kinetic parameters for some of the mutants. Our kinetic study on the G60A mutant indicates that the mutation does not affect the defattyacylase activity. Our results also suggest that Sirt6 auto ADP-ribosylation might be weak when compared to the robust ADP-ribosylation of DT by EF-2. More studies need to be performed to explore whether PARP-1 could be fattyacylated. It would also be interesting to investigate if the auto ADP-ribosyltransferase activity of Sirt6 would increase or decrease the defattyacylase activity. It is also possible that two activities might be independent and would act depending on the context.

REFERENCES

1. Jiang, H., Khan, S., Wang, Y., Charron, G., He, B., Sebastian, C., Du, J., Kim, R., Mostoslavasky, R., Hang, H. C., Hao, Q., and Lin, H., Sirt6 Regulates TNF-α via Hydrolysis of Long Chain Fattyacyl Lysine. *Nature* 496, 110-113, April 4 (2013).
2. Mao, Z., Hine, C., Tian, X., Van Meter, M., Au, M., Vaidya, A., Seluanoy, A., and Gorbunova, V., SIRT6 Promotes DNA Repair under Stress by Activating PARP-1. *Science* 17, 332(6036):1443-6, June (2011).
3. Mao, Z., Hine, C., Tian, X., Van Meter, M., Ke, Z., Seluanoy, A., and Gorbunova, V., Sirtuin 6 (SIRT6) Rescues the Decline of Homologous Recombination Repair during Replicative Senescence. *Proc. Natl. Acad. Sci. U. S. A.* 17, 109 (29):11800-5, July (2012).
4. Liszt, G., Ford, E., Kurtev, M., and Guarente, L., Mouse Sir2 Homolog SIRT6 is a Nuclear ADP-Ribosyltransferase. *J. Biol. Chem.* 3; 280(22); 21313-20, June 3 (2005).
5. Du, J., Jiang, H., and Lin, H., Investigating the ADP-Ribosyltransferase Activity of Sirtuins with NAD Analogs and ^{32}P-NAD. *Biochemistry 48*, 2878-2890 (2009).
6. Stratagene QuikChange II Site-Directed Mutagenesis Kit, available at http://www.genomics.agilent.com/files/MSDS/200523_NAEnglish.pdf.

CHAPTER 4

Conclusion and Future Directions

4.1 Introduction

Sirtuins are NAD-dependent deacetylases. The aim of the present study was to look for an alternate and more efficient activity for one of the seven human sirtuins, Sirt6. Sirt6 has been important in various biological functions including the transcriptional regulation of genes involved in metabolism and inflammation (1, 2), genome stability (3) and lifespan expansion (4). All of these important biological functions are ascribed to the NAD-dependent deacetylase activity of Sirt6. However, the deacetylation activity of Sirt6 is weak when compared to the deacetylation by other members of the sirtuin family, i.e. Sirt1, Sirt2, and Sirt3, which are known for the robust deacetylation of their substrates. The weak deacetylation activity of Sirt6 yet strong biological implications indicated a knowledge gap in the biochemistry of the protein. The main motivation for the present study comes from the work on Sirt5 (5), which suggests that although Sirt5 is a weak deacetylase, it possesses robust desuccinylase and demalonylase activities and that the protein malonylation is a new posttranslational modification. Hence, the aim of this study was to explore an alternate, more robust activity of Sirt6 by investigating whether Sirt6 could hydrolyze any other physiologically relevant modifications on acyl lysine residue. We wanted to achieve this by studying various biochemical parameters such as kinetic parameters and reaction mechanism for the possible alternate activity.

4.2 Empirical Findings

The approach followed in this work was to synthesize a small peptide library using the H3K9 histone peptide sequence as the backbone. Physiologically relevant acyl modifications were added to the lysine K9 side chain and an array of substrates was generated. These substrates were screened with the recombinant Sirt6 in order to check whether Sirt6 could reverse/remove these modifications using various biochemical techniques such as HPLC-MS, MALDI TOF spectroscopy, and biochemical radiolabeling. The synthesized peptide library was also useful later in screening other sirtuins of the same class but different species such as Pfsir2A for a novel activity (6). The major findings of this work include the following:

a) Sirt6 exhibits a preference for removing longer chain fattyacyl modification from the H3K9 peptide backbone in comparison to other physiologically relevant modifications such as biotin, HMG, succinyl, lipoyl, acetyl, and ubiquitinyl.

b) The k_{cat}/K_m for demyristoylation (1400 $s^{-1}M^{-1}$) is roughly 300 fold better than that for deacetylation (4.8 $s^{-1}M^{-1}$). The increased catalytic efficiency comes mainly from the decrease in K_m for the myristoyl peptide. The K_m for deacetylation is 810 µM and for demyristoylation it is 3.4 µM.

c) The novel activity allows Sirt6 to utilize substrates other than the H3K9 acetyl peptide which is in contrast to its highly sequence specific deacetylation activity.

d) The mechanism for the novel Sirt6 demyristoylase activity is the same as that for the deacetylase activity.

e) O´-fattyacyl ADP-ribose intermediate was isolated using the HPLC based assay.

f) The crystal structure of Sirt6 with H3K9 myristoyl peptide and ADP-ribose was obtained, which demonstrated the presence of long hydrophobic acyl pocket preference of Sirt6 for long chain fattyacyl group. (This was a collaborative work done with Yi Wang and Professor Quan Hao.)

g) The kinetic data using HPLC based assay shows that the demyristoylation of TNFα K19 and TNFα K20 myristoyl peptides by Sirt6 is robust.

h) Sirt6 promotes the secretion of TNFα by removing the fattyacyl modification on Lys19 and Lys20 of TNFα. (This was a collaborative work Dr. Hoang Jiang.)

4.3 Significance of This Work

Sirt6 has been previously reported to be a very weak and sequence specific deacetylase. In this work, we have shown that Sirt6 shows low sequence specificity when the lysine residue has fattyacyl modification. Therefore, this novel Sirt6 activity supports the fact that different sirtuins might prefer different acyl lysine modifications (e.g., Sirt5 prefers succinyl/malonyl modifications (5)) and that deacetylation might just be responsible partially for its function. It is a possibility that both deacetylation and defattyacylation activities might be present for Sirt6. Therefore, sirtuins should rather be broadly defined as "NAD-dependent deacylases" rather than just "NAD-dependent deacetylases." Further, the discovery of defattyacylase activity of Sirt6 on protein lysine fattyacylation (here TNFα) gives us a new way to explore this previously less studied PTM (8, 9). Other signaling molecules such as insulin growth factor 1 (IGF-1) might be controlled by similar mechanism (3, 10).

4.4 Future Work

Possible extensions of this work are as follows:

a) The present study does not show which particular hydrophobic amino acid(s) in the catalytic pocket of Sirt6 is/are important for its "defattyacylase" activity. Testing an inactive mutation in enzymatic assays and further in TNFα secretion assays would further prove that the enzymatic activity is directly related to Sirt6 and is not due to an interacting protein activation.

b) Another extension could be to design inhibitors or activators which would specifically inhibit/activate the Sirt6 activity. Since different sirtuins prefer different acyl groups, specific inhibitors or activators could be synthesized for Sirt6. Using these inhibitors and activators, the physiological function of Sirt6 could be studied in greater details at both cellular and organismic level.

REFERENCES

1. Zhong, L., D'Urso, A., Toiber, D., Sebastian, C., Henry, R. E., Vadysirisack, D. D. *et al.*, The Histone Deacetylase Sirt6 Regulates Glucose Homeostasis via Hif1[alpha]. *Cell* 140, 280-293 (2010).
2. Kawahara, T. L., *et al*., SIRT6 Links Histone H3 Lysine 9 Deacetylation to NF-kappaB-Dependent Gene Expression and Organismal Life Span. *Cell* 136, 62-74 (2009)
3. Mostoslavsky, R., Chua, K. F., Lombard, D. B., Pang, W. W., Fischer, M. R., Gellon, L. *et al*., Genomic Instability and Aging-Like Phenotype in the Absence of Mammalian SIRT6. *Cell* 124, 315-329 (2006)
4. Kanfi, Y., Naiman, S., Amir, G., Peshti, V., Zinman, G., Nahum, L., Bar- Joseph, Z., and Cohen, H. Y., The Sirtuin SIRT6 Regulates Lifespan in Male Mice. *Nature* 483, 218-221 (2012)
5. Du, J., Zhou, Y., Su, X., Yu, J. J., Khan, S., Jiang, H., Kim, J., Woo, J., Kim, J. H., Choi, B. H., He, B., Chen, W., Zhang, S., Cerione, R. A., Auwerx, J., Hao, Q., and Lin, H., SirT5 is a NAD-Dependent Protein Lysine Demalonylase and Desuccinylase. *Science* 334, 806–809 (2011).
6. Zhu, A. Y., Zhou, Y., Khan, S., Deitsch, K. W., Hao, Q., and Lin, H., Plasmodium Falciparum Sir2A Preferentially Hydrolyzes Medium and Long Chain Fattyacyl Lysine. *ACS Chem. Biol.* 7, 155-159 (2011).

7. Jiang, H., Khan, S., Wang, Y., Charron, G., He, B., Sebastian, C., Du, J., Kim, R., Mostoslavasky, R., Hang, H. C., Hao, Q., and Lin, H., Sirt6 Regulates TNFα via Hydrolysis of Long Chain Fatty Acyl Lysine. *Nature* 496, 110-113, April 4 (2013).
8. Stevenson, F. T., Bursten, S. L., Fanton, C., Locksley, R. M. & Lovett, D. H. The 31-kDa Precursor of Interleukin 1 Alpha is Myristoylated on Specific Lysines within the 16-kDa N-Terminal Propiece. *Proc. Natl. Acad. Sci. U. S. A.* 90, 7245-7249 (1993).
9. Stevenson, F. T., Bursten, S. L., Locksley, R. M. & Lovett, D. H. Myristoyl Acylation of the Tumor Necrosis Factor Alpha Precursor on Specific Lysine Residues. *J. Exp. Med.* 176, 1053-1062 (1992).
10. Schwer, B., Schumacher, B., Lombard, D. B., Xiao, C., Kurtev, M. V., Gao, J. et al. Neural Sirtuin 6(Sirt6)Ablation Attenuates Somatic Growth and Causes Obesity. *Proc. Natl. Acad. Sci. U.S. A.* 107, 21790-21794 (2010).

APPENDIX A

Permission for Reproduction

1. *Fig. 1.1 reused with permission from*

   Vaquero, A., The Conserved Role of Sirtuins in Chromatin Regulation. *Int. J. Dev. Biol.* 53, 303-322 (2009)

   Copyright @ UBC Press

2. *Fig. 1.2 and Fig. 2.1 reused with permission from*

   Du, J., Zhou, Y., Su, X., Yu, J. J., Khan, S., Jiang, H., Kim, J., Woo, J., Kim, J. H., Choi, B. H., He, B., Chen, W., Zhang, S., Cerione, R. A., Auwerx, J., Hao, Q., and Lin, H., SirT5 is a NAD-Dependent Protein Lysine Demalonylase and Desuccinylase. *Science* 334, 806–809 (2011)

   Copyright @ American Association for the Advancement of Science

3. *Fig. 1.3, Fig. 2.8, Fig. 2.9, Table 2.2, and Table 2.3 reused with permission from*

   Jiang, H., Khan, S., Wang, Y., Charron, G., He, B., Sebastian, C., Du, J., Kim, R., Mostoslavasky, R., Hang, H. C., Hao, Q., and Lin, H., Sirt6 Regulates TNFα via Hydrolysis of Long Chain Fatty Acyl Lysine. *Nature* 496, 110-113, April 4 (2013)

   Copyright @ Nature Publishing Group